

AD-A181 455

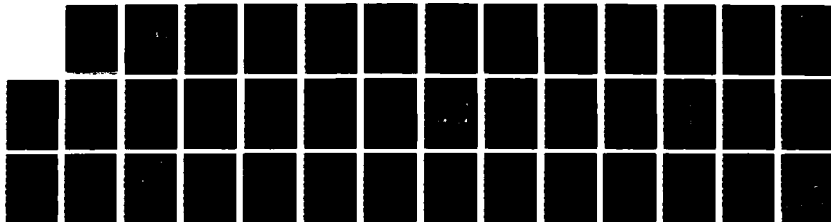
FINITE-DIFFERENCE MODELING OF SEISMOLOGICAL PROBLEMS IN  
MAGNITUDE ESTIMAT (U) TELEDYNE GEOTECH ALEXANDRIA VA  
ALEXANDRIA LABS K L MCLAUGHLIN ET AL MAR 87

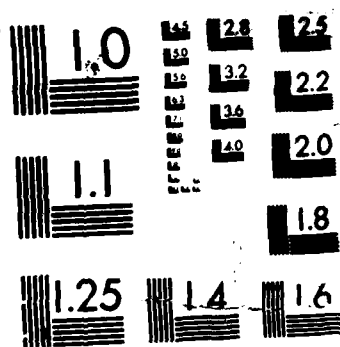
1/1

UNCLASSIFIED

TGAL-87-01 AFGL-TR-87-0106 F19628-85-C-0035 F/G 17/10

NL





MICROCOPY RESOLUTION TEST CHART  
NATIONAL BUREAU OF STANDARDS-1963-A

(12)

DTIC FILE COPY

AD-A181 455

AFGL-TR-87-0106

**FINITE-DIFFERENCE MODELING OF SEISMOLOGICAL PROBLEMS  
IN MAGNITUDE ESTIMATION USING BODY WAVES, SURFACE WAVES  
AND SEISMIC SOURCE IMAGING**

Keith L. McLaughlin  
Zoltan A. Der  
Rong-Song Jih  
Alison C. Lees  
Lisa M. Anderson

Teledyne Geotech Alexandria Laboratories  
314 Montgomery Street  
Alexandria, VA 22314-1581

DTIC  
ELECTE  
JUN 19 1987  
S D D

MARCH 1987

FINAL REPORT

11 February 1985 --- 10 February 1987

APPROVED FOR PUBLIC RELEASE; DISTRIBUTION UNLIMITED

AIR FORCE GEOPHYSICS LABORATORY  
AIR FORCE SYSTEMS COMMAND  
UNITED STATES AIR FORCE  
HANSCOM AIR FORCE BASE, MASSACHUSETTS 01731

"This technical report has been reviewed and is approved for publication"

  
JAMES F. LEWKOWICZ  
Contract Manager

  
HENRY A. OSSING  
Branch Chief

FOR THE COMMANDER

  
DONALD H. ECKHARDT  
Division Director

This report has been reviewed by the ESD Public Affairs Office (PA) and is releasable to the National Technical Information Service (NTIS).

Qualified requestors may obtain additional copies from the Defense Technical Information Center. All others should apply to the National Technical Information Service.

If your address has changed, or if you wish to be removed from the mailing list, or if the addressee is no longer employed by your organization, please notify AFGL/DAA, Hanscom AFB, MA 01731. This will assist us in maintaining a current mailing list.

Do not return copies of this report unless contractual obligations or notices on a specific document requires that it be returned.

## REPORT DOCUMENTATION PAGE

AD-A161 755

Form Approved  
OMB No 0704-0188  
Exp Date Jun 30, 1986

1a REPORT SECURITY CLASSIFICATION Unclassified			1b RESTRICTIVE MARKINGS	
2a SECURITY CLASSIFICATION AUTHORITY			3 DISTRIBUTION/AVAILABILITY OF REPORT approved for public release; distribution unlimited	
2b DECLASSIFICATION/DOWNGRADING SCHEDULE				
4 PERFORMING ORGANIZATION REPORT NUMBER(S) TGAL-87-01			5 MONITORING ORGANIZATION REPORT NUMBER(S) AFGL-TR-87- 0106	
6a NAME OF PERFORMING ORGANIZATION Teledyne Geotech		6b OFFICE SYMBOL (if applicable) TGAL		7a NAME OF MONITORING ORGANIZATION Air Force Geophysics Laboratory
6c ADDRESS (City, State, and ZIP Code) 314 Montgomery Street Alexandria, VA 22314-1581			7b ADDRESS (City, State, and ZIP Code) Hanscom AFB MA 01731-0035	
8a NAME OF FUNDING / SPONSORING ORGANIZATION Air Force Geophysics Laboratory		8b OFFICE SYMBOL (if applicable) DSO/GSD		9 PROCUREMENT INSTRUMENT IDENTIFICATION NUMBER F19628-85C-0035
8c ADDRESS (City, State, and ZIP Code) Hanscom AFB MA 01731-5000			10 SOURCE OF FUNDING NUMBERS PROGRAM ELEMENT NO 62714E	
			PROJECT NO 5A10	TASK NO DA
			WORK UNIT ACCESSION NO AX	
11 TITLE (Include Security Classification) Finite-Difference Modeling of Seismological Problems in Magnitude Estimation using Body Waves, Surface Waves, and Seismic Source Imaging				
12 PERSONAL AUTHOR(S) K. L. McLaughlin, Z. A. Der, R.-S. Jih, A. C. Lees, and L. M. Anderson				
13a TYPE OF REPORT Final Report		13b TIME COVERED FROM 2/11/85 to 2/10/87		14 DATE OF REPORT (Year, Month, Day) March 1987
15 PAGE COUNT 38				
16 SUPPLEMENTARY NOTATION				
17 COSATI CODES FIELD      GROUP      SUB-GROUP			18 SUBJECT TERMS (Continue on reverse if necessary and identify by block number) Finite-Difference      Synthetics      Scattering Heterogeneity      Topography	
19 ABSTRACT (Continue on reverse if necessary and identify by block number) <p>We briefly summarize in this final report the results from the three scientific reports delivered under this contract. Our work has focused on the effects of near-source heterogeneity upon seismic magnitude-yield determination. The basic tool in this work has been a developing 2-dimensional linear finite-difference code which computes the dynamic elastic response of an Earth model to specified initial conditions. By use of various initial conditions and the reciprocity theorem, we can generate the linear response of the Earth model to a general seismic source. Current work is limited to 2-D models and line sources. This FORTRAN-77 code has been run under the UNIX operating system on VAX, Cray, SUN, and Celerity. Major modifications on the code during this project include the addition of general free-surface boundary conditions capable of handling topography with slopes of any angle, as well as the fundamental mode Rayleigh wave packet adequate for numerical studies. Work on this program continues to increase it's performance, versatility, and portability.</p>				
20 DISTRIBUTION/AVAILABILITY OF ABSTRACT <input type="checkbox"/> UNCLASSIFIED/UNLIMITED <input type="checkbox"/> SAME AS RPT <input type="checkbox"/> DTIC USERS			21 ABSTRACT SECURITY CLASSIFICATION Unclassified	
22a NAME OF RESPONSIBLE INDIVIDUAL James F. Lewkowitz			22b TELEPHONE (Include Area Code) (617) 377-3028	22c OFFICE SYMBOL LWH

(19. Continued)

Finite-difference simulations of P wave propagation through models of extreme topographic profiles of the southern Sahara test site were used to investigate the effect of topography on the variation of short-period  $m_b$  estimate of contained nuclear explosions. We have shown, as much as the 2-D assumption is valid, that the topography above the explosions RUBIS and SAPHIR could be responsible for suppressing the elastic pP. As part of the data analysis to support these calculations we have refined the attenuation estimate (spectral  $t^*$  estimate) for the southern Sahara test site and confirm that the attenuation bias between this test site and NTS should be minimal. Furthermore, we have used both spectral and deconvolution techniques to estimate far-field P-wave source time functions and explosion moments for SAPHIR, RUBIS, EMERAUDE, and GRENAT.

Synthetic teleseismic P-wave seismograms were also produced for a two dimensional, laterally heterogeneous model of Yucca Flats, NTS. This work shows that the geologic structure of Yucca Flats could be responsible for generation of the reverberant P coda and for teleseismic magnitude variations as large as 0.3 magnitude units. This structure would also make difficult the identification of elastic P+pP interference in the frequency domain. Indications are that  $m_b$  magnitude variations should be reduced by averaging over many azimuths and takeoff angles at teleseismic distance.

Finite-difference simulations were used to investigate the scattering of incident Rayleigh waves. Shallow explosions in layered media generate considerable more short-period Rayleigh wave energy than is observed, so the Rayleigh waves must be either attenuated by absorption or scattering. We find that reflection of Rayleigh waves by topographic features is an inefficient process and the bulk of the energy that is not transmitted as Rayleigh waves is converted to bodywaves. The scattering of these short-period Rayleigh waves into SV trapped in the crust as Lg or as P waves scattered into teleseismic P coda serve as possible models for the generation of Lg by explosions and the generation of teleseismic P coda near the source. Future work along this line is to compare the scattering from topography to that produced by shallow heterogeneity.

Recommendations for further work include:

- (1) Extensions of the current finite difference code from 2-D to 3-D to study the attenuation of body waves by 3-D heterogeneity in the crust, test hypotheses about the generation of P coda and anisotropic P wave generation, and generation of transverse Lg by explosions.
- (2) Introduction of other numerical methods to explore the coupling (scattering) of modes of wave-guide regional phases such as Pg and Lg, as well as the scattering of Pn and Sn. These methods include 2-D and 3-D scattering from localized heterogeneity as well as from rough boundaries.
- (3) Coupling of efficient reflectivity methods to finite difference calculations to propagate the scattered field to regional distances and to drive the finite difference responses with realistic in-coming regional phases.
- (4) Investigation of scattering of fundamental and higher mode short-period Rayleigh waves by 2-D topography and shallow heterogeneity with more realistic velocity gradients near the surface.
- (5) Extension of the general topographic boundary condition to include the general fluid-solid interface for the modeling of scattering at rough fluid-solid boundaries.

## SUMMARY

We briefly summarize in this final report the results from the three scientific reports delivered under this contract. Our work has focused on the effects of near-source heterogeneity upon seismic magnitude-yield determination. The basic tool in this work has been a developing 2-dimensional linear finite-difference code which computes the dynamic elastic response of an Earth model to specified initial conditions. By use of various initial conditions and the reciprocity theorem, we can generate the linear response of the Earth model to a general seismic source. Current work is limited to 2-D models and line sources. This FORTRAN-77 code has been run under the UNIX operating system on VAX, Cray, SUN, and Celerity. Major modifications on the code during this project include the addition of general free-surface boundary conditions capable of handling topography with slopes of any angle, as well as the fundamental mode Rayleigh wave packet adequate for numerical studies. Work on this program continues to increase its performance, versatility, and portability.

Finite-difference simulations of P wave propagation through models of extreme topographic profiles of the southern Sahara test site were used to investigate the effect of topography on the variation of short-period  $m_b$  estimate of contained nuclear explosions. We have shown, as much as the 2-D assumption is valid, that the topography above the explosions RUBIS and SAPHIR could be responsible for suppressing the elastic pP. As part of the data analysis to support these calculations we have refined the attenuation estimate (spectral  $\bar{r}^*$  estimate) for the southern Sahara test site and confirm that the attenuation bias between this test site and NTS should be minimal. Furthermore, we have used both spectral and deconvolution techniques to estimate far-field P-wave source time functions and explosion moments for SAPHIR, RUBIS, EMERAUDE, and GRENAT.

<input checked="" type="checkbox"/>	
<input type="checkbox"/>	
<input type="checkbox"/>	
Codes	
and/or Special	
A-1	



Synthetic teleseismic P-wave seismograms were also produced for a two dimensional, laterally heterogeneous model of Yucca Flats, NTS. This work shows that the geologic structure of Yucca Flats could be responsible for generation of the reverberant P coda and for teleseismic magnitude variations as large as 0.3 magnitude units. This structure would also make difficult the identification of elastic P+pP interference in the frequency domain. Indications are that  $m_b$  magnitude variations should be reduced by averaging over many azimuths and takeoff angles at teleseismic distance.

Finite-difference simulations were used to investigate the scattering of incident Rayleigh waves. Shallow explosions in layered media generate considerable more short-period Rayleigh wave energy than is observed, so the Rayleigh waves must be either attenuated by absorption or scattering. We find that reflection of Rayleigh waves by topographic features is an inefficient process and the bulk of the energy that is not transmitted as Rayleigh waves is converted to bodywaves. The scattering of these short-period Rayleigh waves into SV trapped in the crust as Lg or as P waves scattered into teleseismic P coda serve as possible models for the generation of Lg by explosions and the generation of teleseismic P coda near the source. Future work along this line is to compare the scattering from topography to that produced by shallow heterogeneity.

Recommendations for further work include:

- (1) Extensions of the current finite difference code from 2-D to 3-D to study the attenuation of body waves by 3-D heterogeneity in the crust, test hypotheses about the generation of P coda and anisotropic P wave generation, and generation of transverse Lg by explosions.
- (2) Introduction of other numerical methods to explore the coupling (scattering) of modes of wave-guide regional phases such as Pg and Lg, as well as the scattering of Pn and Sn.

These methods include 2-D and 3-D scattering from localized heterogeneity as well as



from rough boundaries.

- (3) Coupling of efficient reflectivity methods to finite difference calculations to propagate the scattered field to regional distances and to drive the finite difference responses with realistic in-coming regional phases.
- (4) Investigation of scattering of fundamental and higher mode short-period Rayleigh waves by 2-D topography and shallow heterogeneity with more realistic velocity gradients near the surface.
- (5) Extension of the general topographic boundary condition to include the general fluid-solid interface for the modeling of scattering at rough fluid-solid boundaries.

## TABLE OF CONTENTS

	Page
SUMMARY	iii
1. BOUNDARY CONDITIONS FOR ARBITRARY POLYGONAL TOPOGRAPHY IN A 2-D ELASTIC FINITE-DIFFERENCE SCHEME FOR SEISMOGRAM GENERATION (Section 1 of AFGL-TR-86-0159, <i>Scientific Report #1, TGAL-86-03</i> ) (available through NTIS)	1
2. TELESEISMIC SPECTRAL AND TEMPORAL $M_0$ AND $\Psi_\infty$ ESTIMATES FOR FOUR FRENCH EXPLOSIONS IN SOUTHERN SAHARA (Section 2 of AFGL-TR-86-0159, <i>Scientific Report #1, TGAL-86-03</i> ) (available through NTIS)	5
3. SCATTERING FROM NEAR-SOURCE TOPOGRAPHY: TELESEISMIC OBSERVATIONS AND NUMERICAL 2-D EXPLOSIVE LINE SOURCE SIMULATIONS (Section 3 of AFGL-TR-86-0159, <i>Scientific Report #1, TGAL-86-03</i> ) (available through NTIS)	10
4. EFFECTS OF LOCAL GEOLOGIC STRUCTURE ON YUCCA FLATS, NTS, EXPLOSION WAVEFORMS: 2-DIMENSIONAL LINEAR FINITE DIFFERENCE SIMULATIONS (AFGL-TR-86-0220, <i>Scientific Report #2, TGAL-86-04</i> ) (available through NTIS)	15
5. FINITE-DIFFERENCE SIMULATIONS OF RAYLEIGH WAVE SCATTERING BY 2-D ROUGH TOPOGRAPHY (AFGL-TR-86-0269, <i>Scientific Report #3, TGAL-86-09</i> ) (available through NTIS)	20

## BOUNDARY CONDITIONS FOR ARBITRARY POLYGONAL TOPOGRAPHY IN A 2-D ELASTIC FINITE-DIFFERENCE SCHEME FOR SEISMOGRAM GENERATION

Rong-Song Jih, Keith L. McLaughlin, and Zoltan A. Der  
Teledyne Geotech Alexandria Laboratories  
314 Montgomery Street  
Alexandria, Virginia 22314-1581

### ABSTRACT

A simple method to implement the free-surface topography of polygonal shape in 2-D explicit finite-difference simulations of the elastic wave equation is presented that includes an empirically stable treatment of various slopes and transition points between the sloping segments.

On the inclined free surface, the vanishing stress conditions are implemented to a rotated coordinate system parallel to the inclined boundary as previous works did. While for each transition point on the topography where the slope changes, we propose to use the first-order approximation of boundary conditions in a locally rotated coordinate system in which the normal axis always coincides with the bisector of the corner. This mixed algorithm is stable for Poisson ratios of practical interest and thus enables us to study a wide range of problems where the topography plays a significant role in shaping the wavefield. Examples are shown simulating the propagation of P and Rayleigh waves traveling through a model with a 45° ramp and a mountain shape as the free surface. By using reciprocity principle and appropriate deconvolutions on the seismograms generated in this scheme, the effect of complicated near-source topography on the far-field teleseismic waveforms can be characterized.

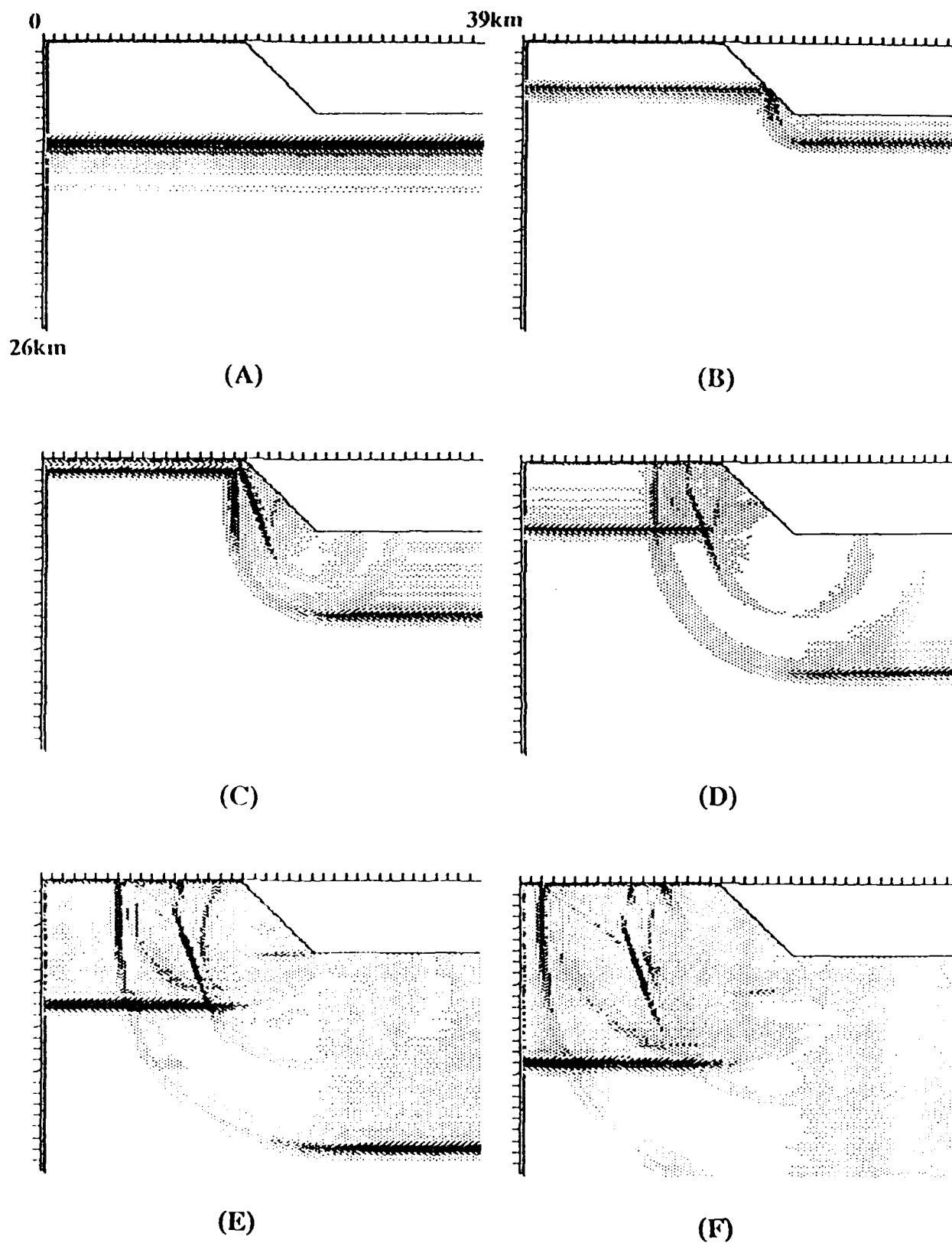
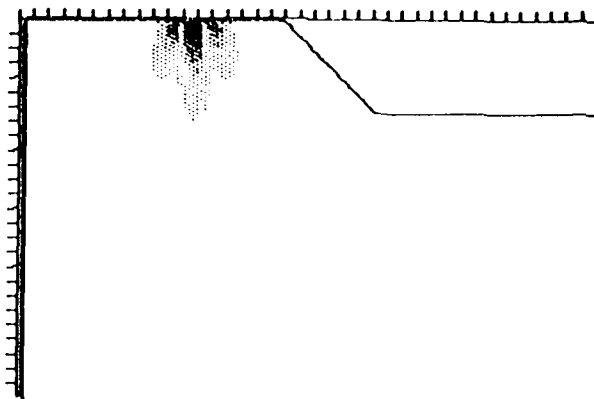
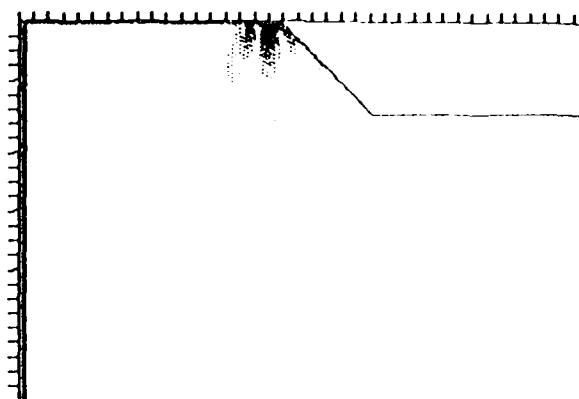


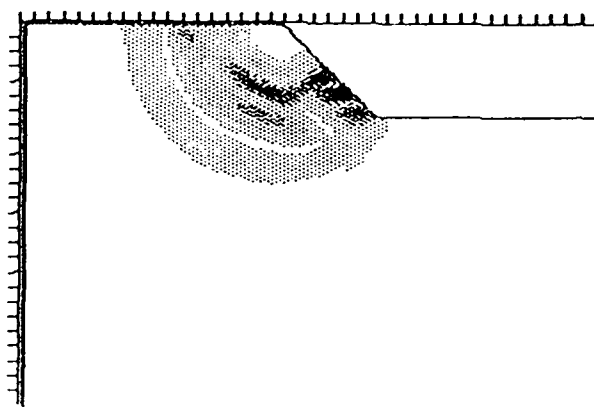
Figure 1.1 The propagation of a normally incident broadband plane P wave through a model with a 45° ramp on the top of grid and symmetric boundary condition used on both sides. Shading is proportional to displacement amplitude. The appropriate P-S conversions and reflections, diffractions satisfying Snell's law and Huygen's principle are clearly visible in these successive snapshots taken every second.



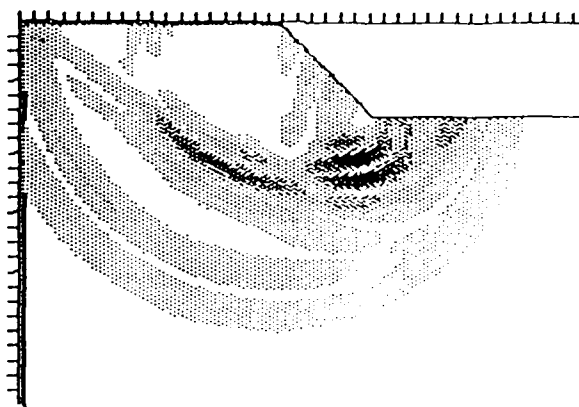
(A)



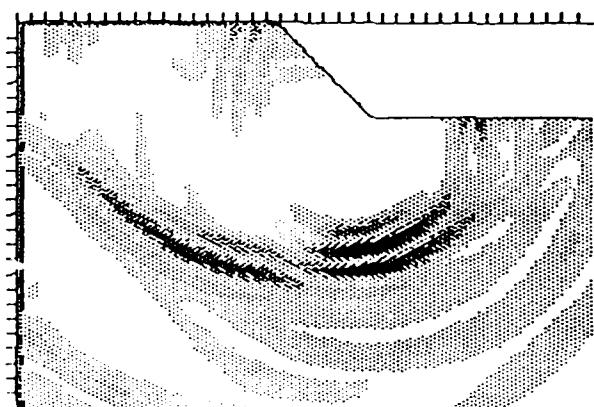
(B)



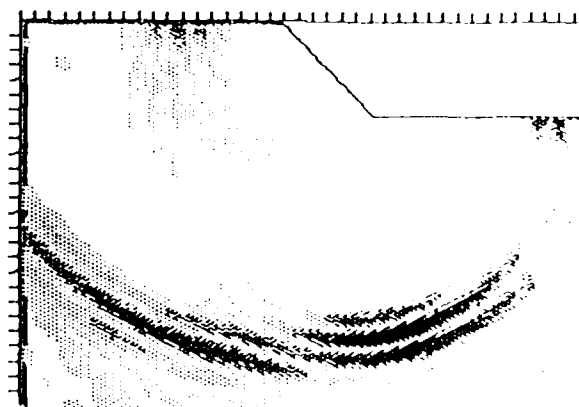
(C)



(D)

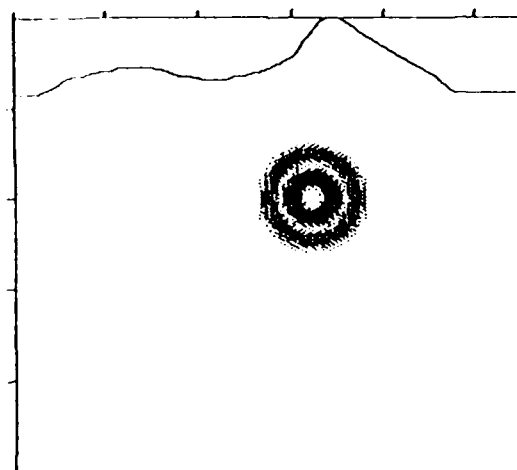


(E)

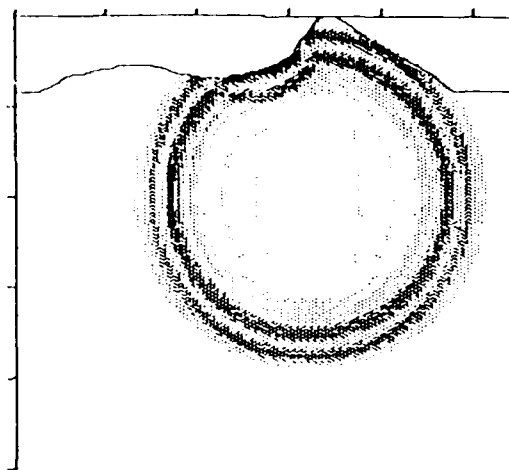


(F)

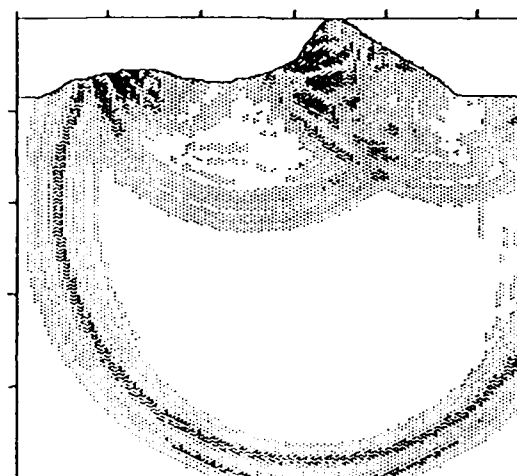
Figure 1.2 Same topographic configuration as in Figure 1.1 with Ricker wavelet-shaped Rayleigh wave of fundamental mode propagating from left side of the grid. When the incident wave packet encounters the corner points of the ramp, the diffraction patterns look like radiation due to point source at corners. Most energy of the incident Rayleigh wave is scattered as body waves and absorbed by the quasi-transparent boundary conditions used in this simulation.



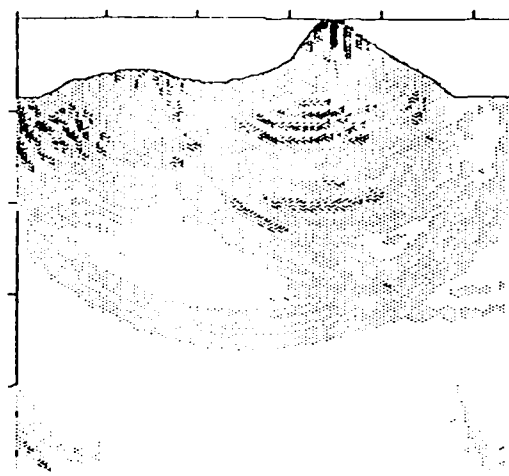
(A)



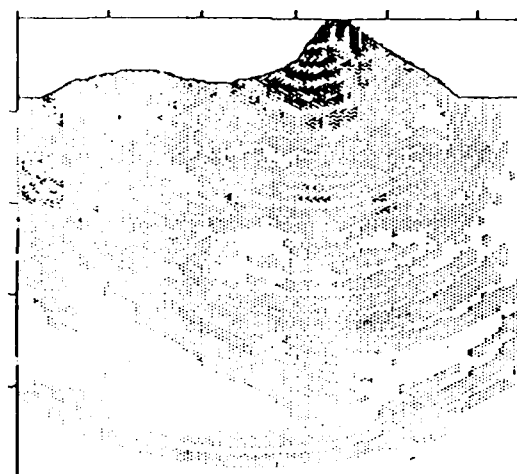
(B)



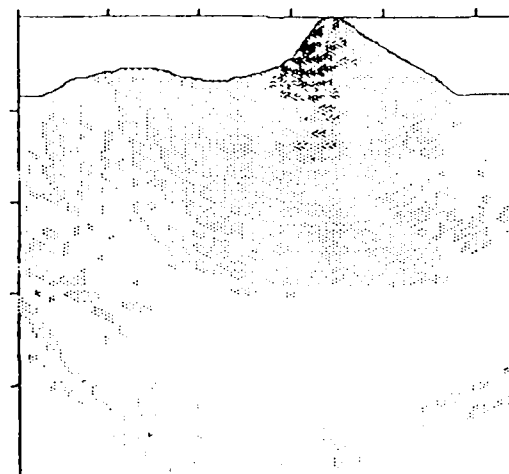
(C)



(D)



(E)



(F)

Figure 1.3 shows the propagation of a compressional point (line) source located beneath a steep topographic profile. Note that the quasi-transparent boundary conditions allow the wave to disappear into the sides and bottom of the grid. Snapshots are separated by 0.25 second.

**TELESEISMIC SPECTRAL AND TEMPORAL  
 $M_o$  AND  $\Psi_\infty$   
ESTIMATES FOR FOUR FRENCH  
EXPLOSIONS IN SOUTHERN SAHARA**

Keith L. McLaughlin, Alison C. Lees, and Zoltan A. Der  
Teledyne Geotech Alexandria Laboratories  
314 Montgomery Street  
Alexandria, Virginia 22314-1581

**ABSTRACT**

Estimates for explosion moment,  $M_o$ , and reduced displacement potential,  $\Psi_\infty$ , are made for four French explosions at Taourirt Tan Afella Massif in southern French Sahara using data from the LRSM network and the arrays EKA and YKA. Preparatory to determining moments,  $\bar{t}^*$  estimates are made for each station and the source region  $\bar{t}^*$  values of 0.30 to 0.35 seconds are found for the southern Sahara test site. This source region attenuation level is consistent with the "hot spot" hypothesis for the Ahaggar plateau in northern Africa. Consequently, the attenuation bias between Ahaggar and the Nevada Test Site should be small.

Both spectral estimation and broadband temporal deconvolution methods are used for estimation of the explosion moments. The deconvolution estimates of static moment are found to be consistent with the spectral estimation methods. Deconvolved seismograms for the explosions EMERAUDE, RUBIS, SAPHIR, and GRENAT show evidence of strong anisotropic free surface interaction that may be due to scattering from the steep topography of the Taourirt Tan Affela Massif test site.

LRSM SPECTRAL MOMENT ESTIMATES $10^{24}$ dyne-cm				
EVENT	MEAN	RMS	GEOMETRIC MEAN	MEDIAN
RUBIS	0.064(0.01)	0.072	0.056	0.059
SAPHIR	0.30(0.10)	0.42	0.19	0.16

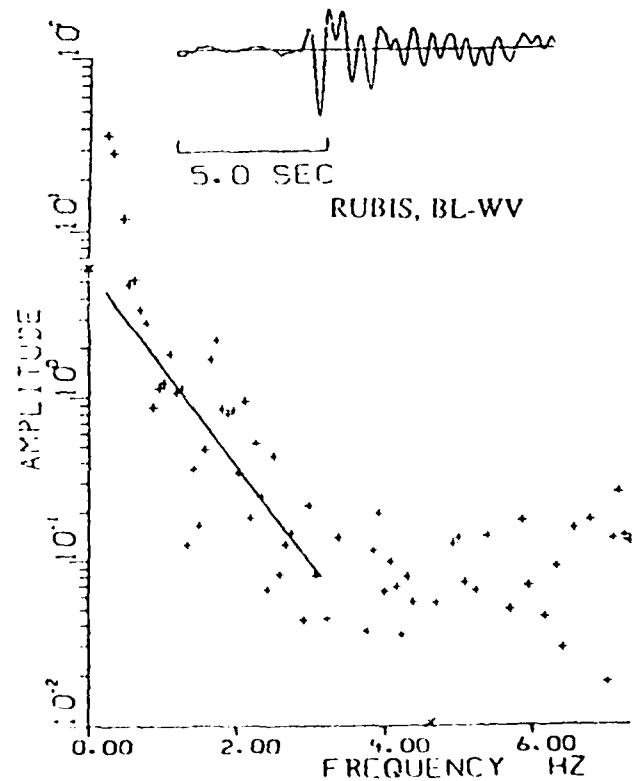
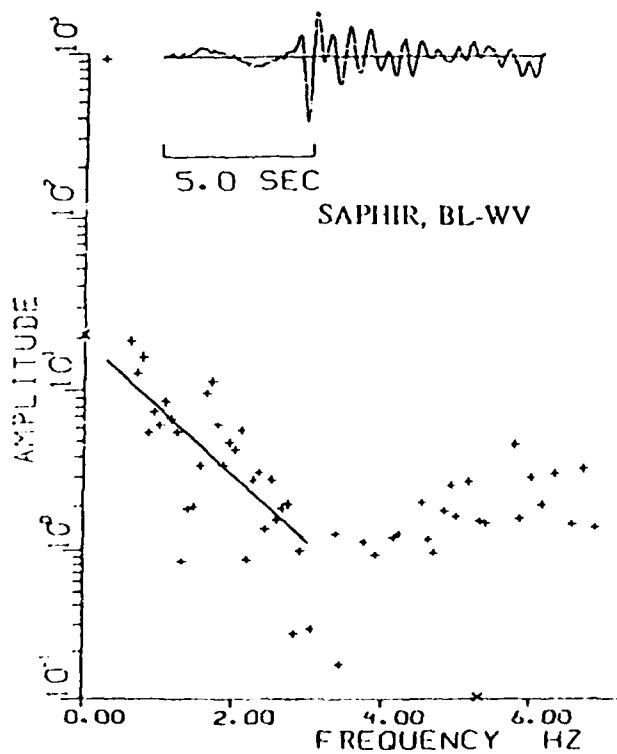
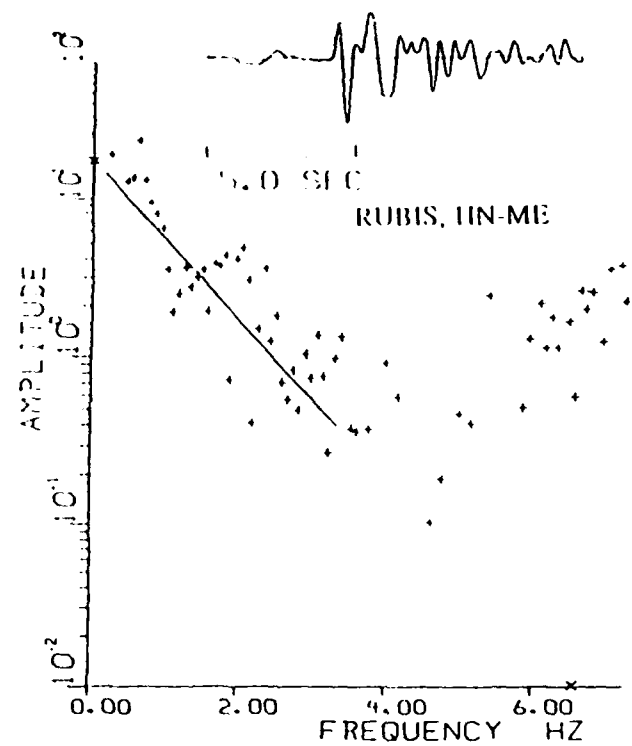
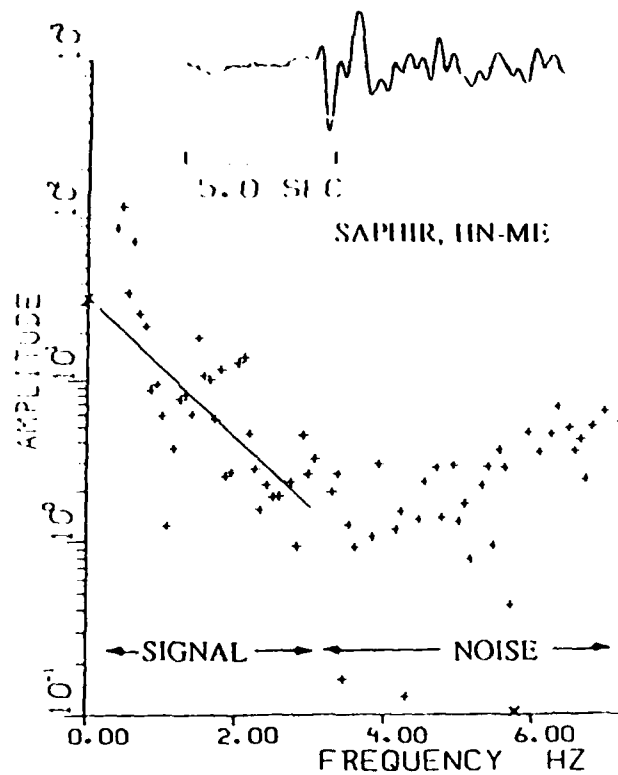


Figure 2.1 Spectra corrected for instrument and RDP. Slopes between 0.5 and 3.0 Hz are estimates of  $r^*$ , intercepts are estimates of  $\Omega_0$ . Only spectral levels with an estimated signal-to-noise power ratio greater than 2 were used.



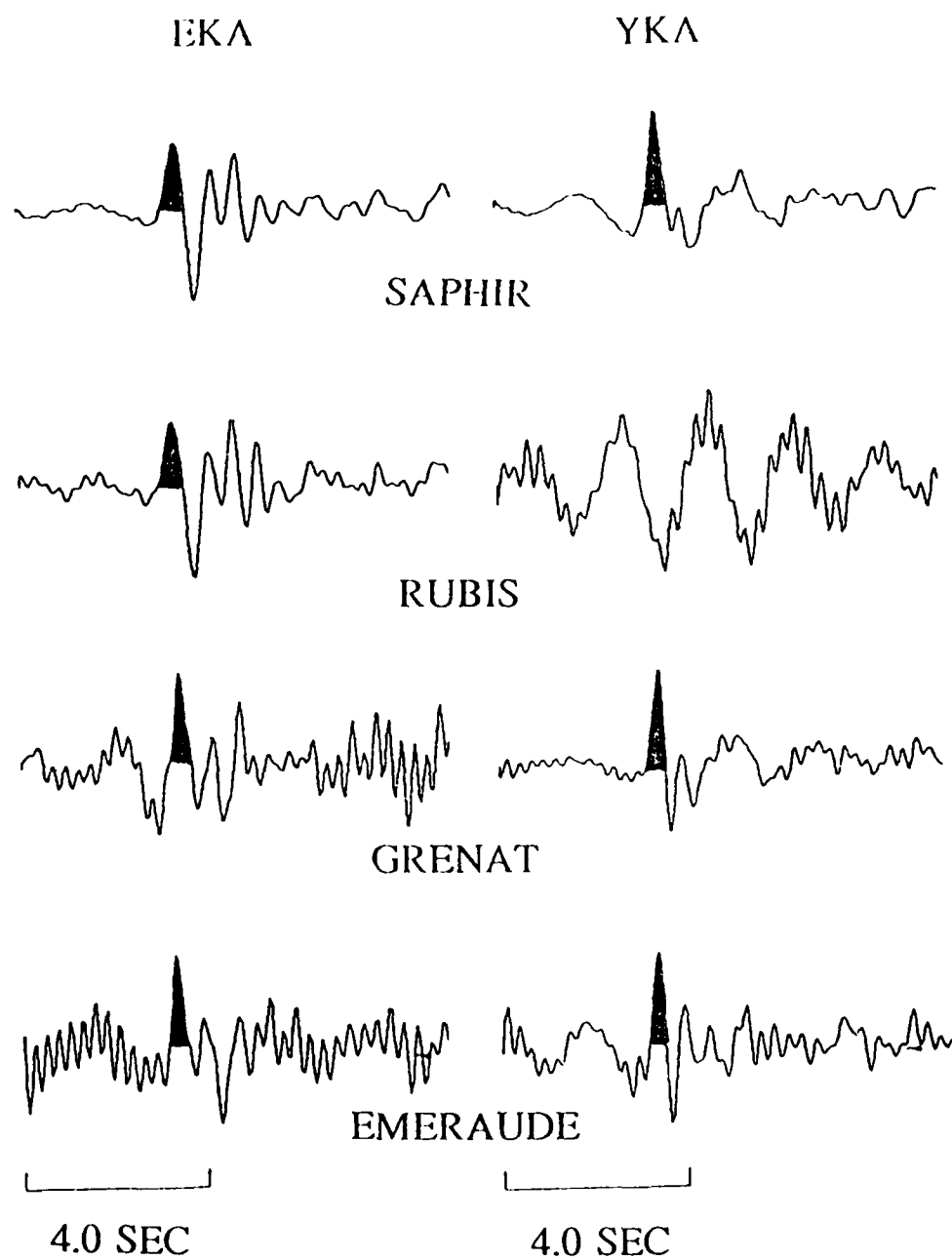


Figure 2.2 Deconvolved source time functions at the EKA and YKA arrays for SAPHIR, RUBIS, GRENAT and EMERAUDE. RUBIS was poorly recorded across YKA.

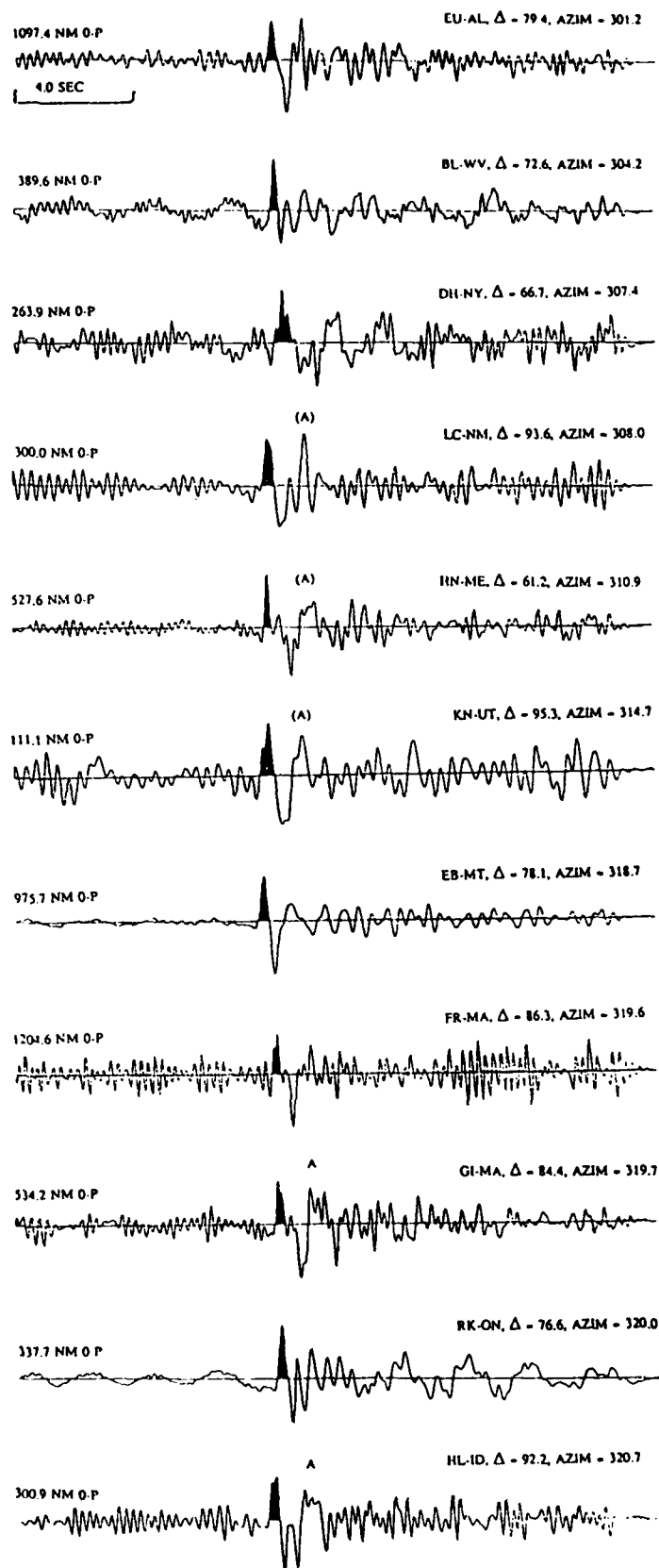


Figure 2.3 Deconvolved waveforms for RUBIS at LRSM stations. The causal P-wave pulse area is indicated for each trace. Traces are ordered in decreasing azimuth from the top. Late positive arrivals that may be correlated between stations are indicated by labels "A" and "(A)".

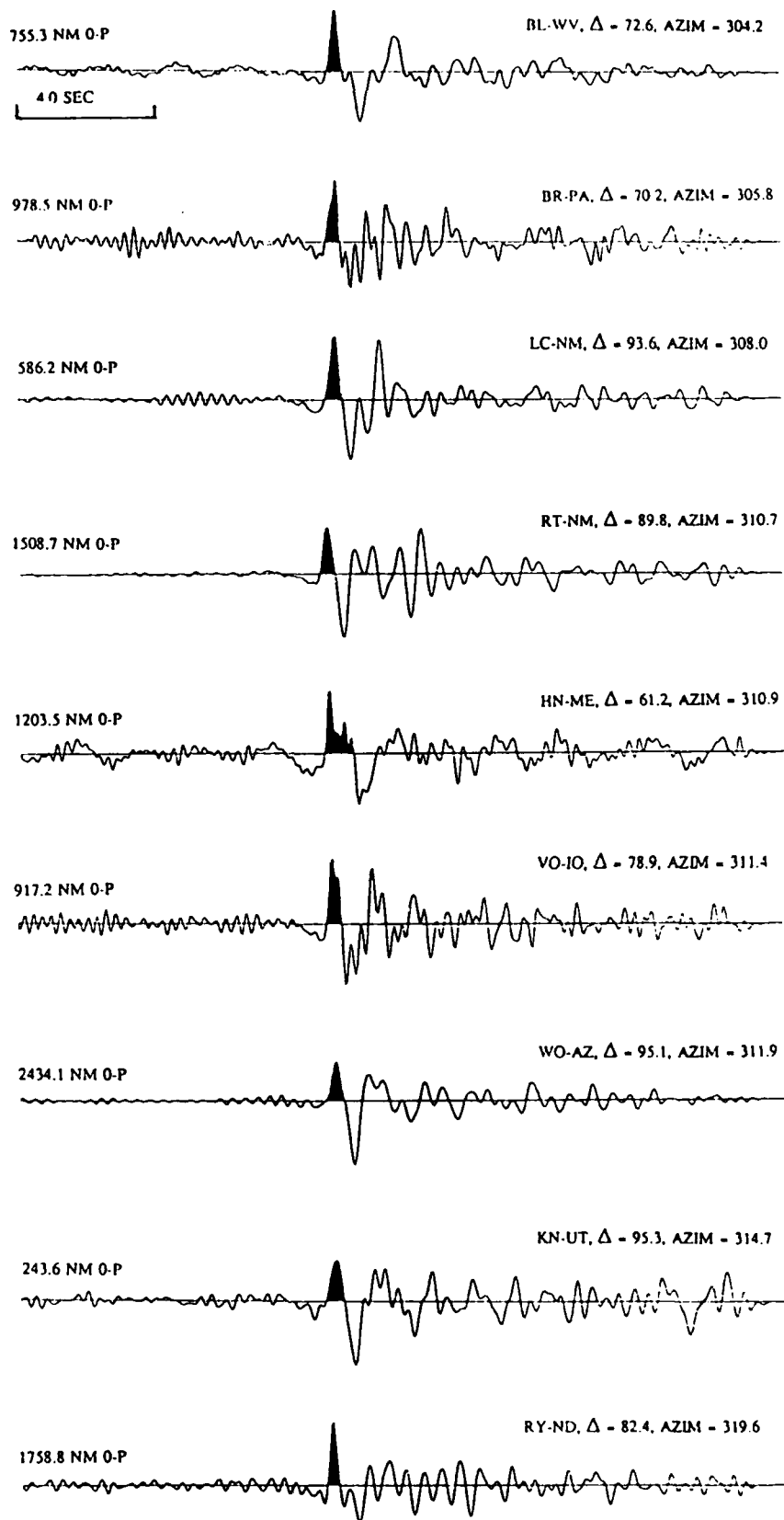


Figure 2.4 Deconvolved waveforms for SAPHIR at LRSM stations. The causal P-wave pulse area is indicated for each trace. Traces are ordered in decreasing azimuth from the top. The HN-ME waveform shows considerable broadening that may be due to a positive secondary arrival unique to the HN-ME station.

**SCATTERING FROM NEAR-SOURCE TOPOGRAPHY:  
TELESEISMIC OBSERVATIONS AND  
NUMERICAL 2-D EXPLOSIVE LINE SOURCE SIMULATIONS**

Keith Lynn McLaughlin and Rong-Song Jih  
Teledyne Geotech Alexandria Labs  
314 Montgomery Street  
Alexandria, Virginia 22314-1581

**ABSTRACT**

2-D linear elastic finite-difference simulations of teleseismic P waveforms from line sources have been used to explore the variations that may be induced in event magnitude-yield determination by the emplacement of explosive sources under mountainous topographic features. The southern Sahara French test site in Algeria, at Taourirt Tan Afella Massif on the Ahaggar plateau has been used as a case study. The topography of this test site is extreme and the event locations permit a test of the hypothesis that topography influences short-period event magnitudes of contained nuclear explosions. The maximum variation that is expected is plus or minus 0.15 magnitude units from the network mean. The magnitude variations are expected to change rapidly with takeoff angle and azimuth.

Teleseismic observations of the explosions at the southern Sahara test site are compared to predictions made from 2-D simulations. Waveform data from the arrays EKA, and YKA as well as LRSM data have been deconvolved to broadband displacement for inspection of the apparent far-field P-wave source. Qualitative comparisons are favorable that the topography above the explosions RUBIS and SAPHIR defocused teleseismic pP at certain takeoff angles and azimuths. Long-period positive-polarity pulses can be seen at several sites that may indicate Rayleigh-to-P scattering from topography near the source.

WWSSN maximum likelihood magnitude data for the "a", "ab", and "max" P phases have been used to estimate that the magnitude variation due to topographic scattering is no more than 0.15 rms magnitude units across the WWSSN.

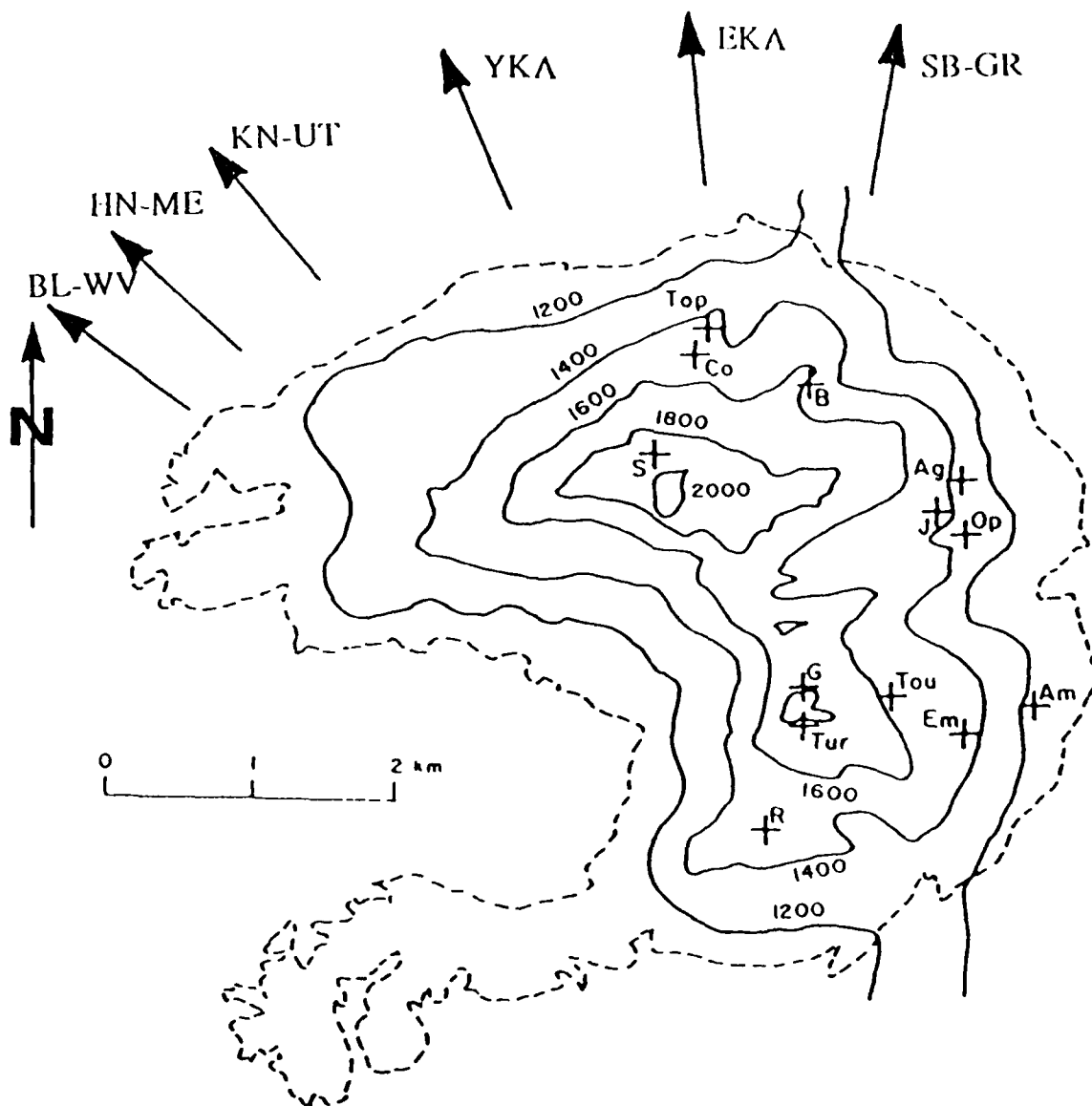
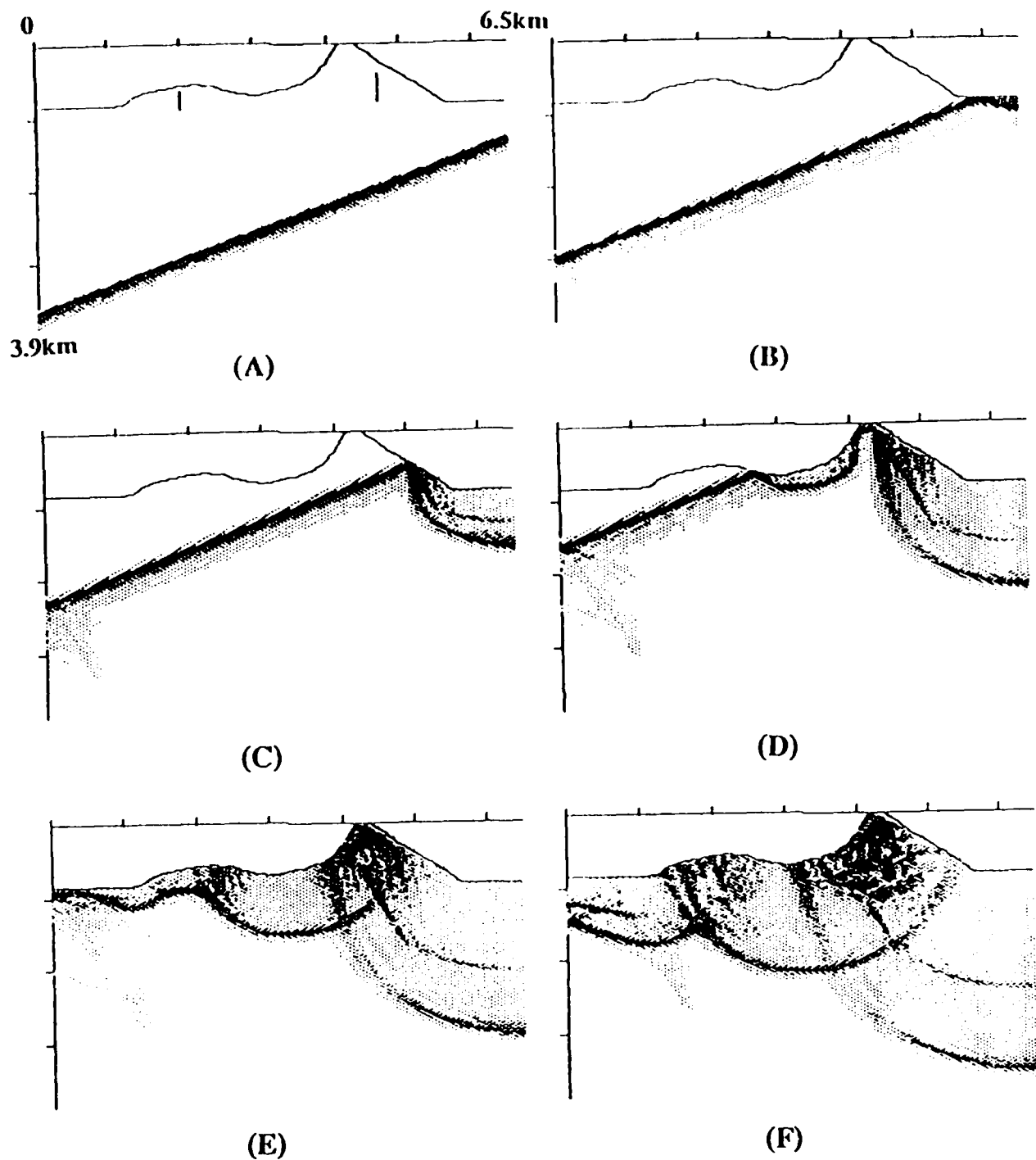


Figure 3.1 Topographic map Taourirt Tan Afella Massif from Duclaux and Michaud (1970) with event locations from Faure (1972) for SAPHIR (S), RUBIS (R), EMERAUDE (E), and GRENAT (G). Contours are 100 meters. The dashed line is the outcrop of the Taourirt Tan Afella Massif granite. Azimuths to several stations and arrays are indicated.



**Figure 3.2** The displacement fields generated by a broadband plane P wave (*i.e.* source at infinity) of incidence angle  $20^\circ$  in a grid with steep topographic configuration. The topography is a (due north  $344^\circ$ ) cross section of Taourirt Tan Afella Massif in southern Algeria. The successive frames separated by 0.125 sec show the initialization of the wave (A), P-reflection followed by S wave starting at right (B,C), completely developed reflections from all parts of the topography (E) and complex wavefields containing reflections, diffractions and possibly excited surface waves (E,F). It can be observed that the free-surface reflection is severely altered due to scattering from the free-surface. Far-field seismograms with compressional sources at locations beneath this topographic profile (black spots in (A)) can be derived by reciprocity.

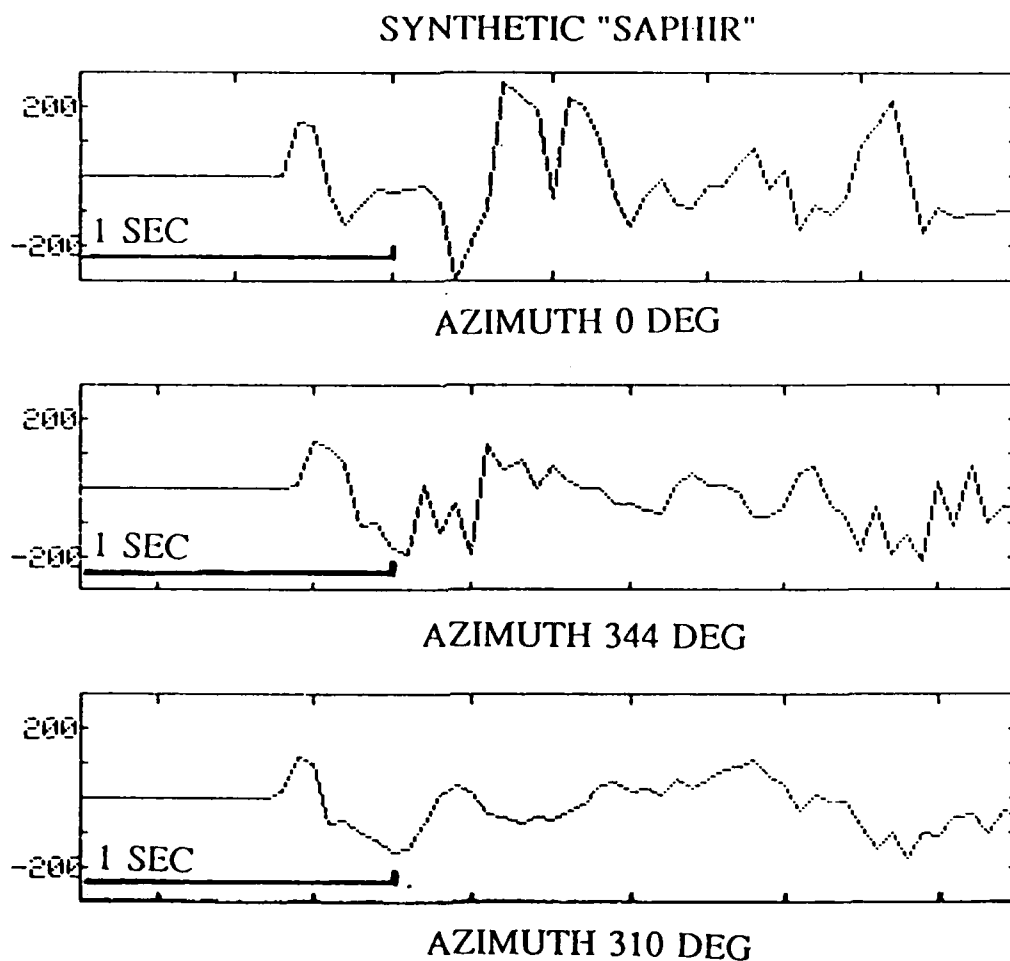


Figure 3.3 Synthetic teleseismic P waves (takeoff angle of 20 degrees) for the 2-D "SAPHIR" models at azimuths of 310, 344, and 0 degrees. Synthetics have only been convolved with an explosion source time function. No distinct well defined elastic pP is apparent although, several long-period complicated negative pulses can be seen to follow the initial P wave. Large positive secondary arrivals can be seen 0.5 sec following the initial P wave at 0 degrees azimuth.

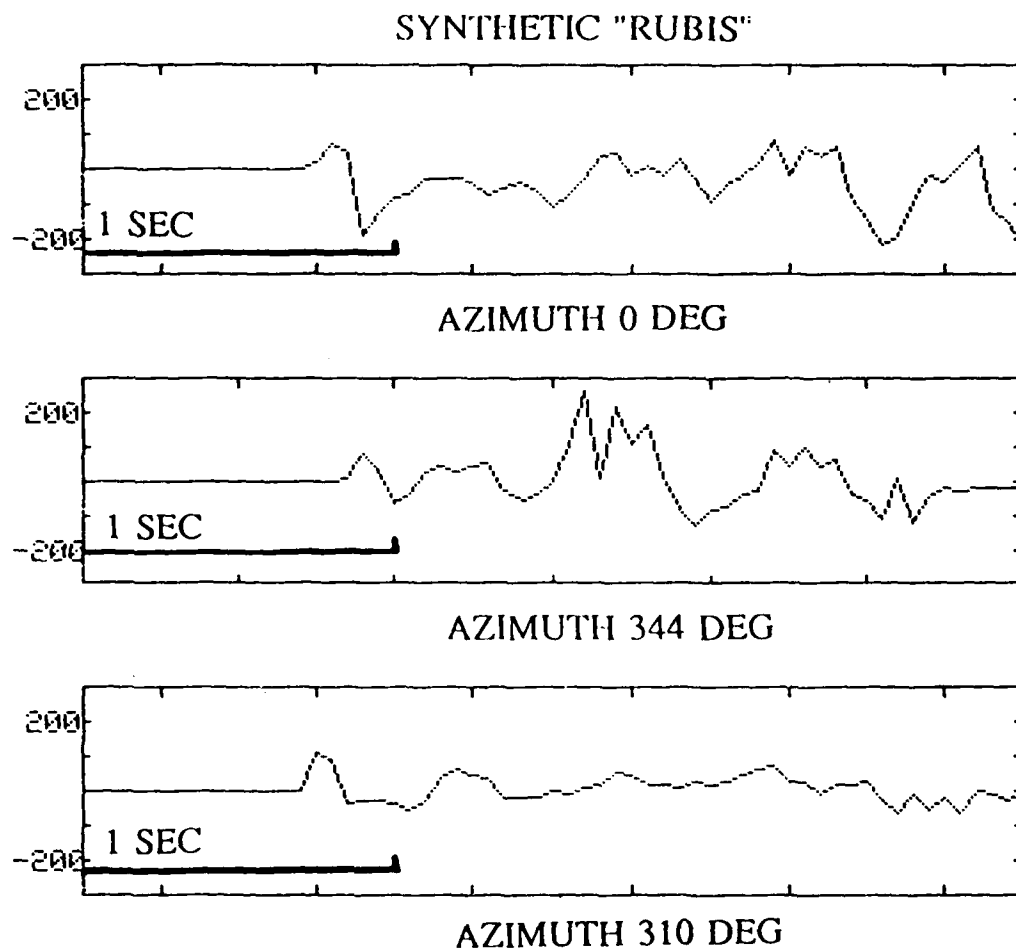


Figure 3.4 Synthetic teleseismic P waves (takeoff angle of 20 degrees) for the 2-D "RUBIS" models at azimuths of 310, 344, and 0 degrees. Synthetics have only been convolved with an explosion source time function. A distinct well defined elastic pP is only apparent for the azimuth of 0 degrees. Large positive pulses can be seen about 1 second after the P wave for the azimuth of 344 degrees.



**EFFECTS OF LOCAL GEOLOGIC STRUCTURE  
ON YUCCA FLATS, NTS, EXPLOSION WAVEFORMS:  
2-DIMENSIONAL LINEAR FINITE-DIFFERENCE SIMULATIONS**

Keith L. McLaughlin, Lisa M. Anderson, and Alison C. Lees  
Teledyne Geotech Alexandria Laboratories  
314 Montgomery Street  
Alexandria, Virginia 22314-1581

**ABSTRACT**

Two-dimensional linear elastic finite-difference calculations were performed for a two-dimensional geologic model of Yucca Flats, Nevada Test Site, Nevada. The calculations were used to produce synthetic teleseismic P-wave seismograms for explosive line sources in Yucca Flats. P-wave coda (first 5 seconds) is observed to be highly dependent on takeoff angle for the teleseismic synthetics. P-wave coda also varies with the position of the source in the valley structure and may produce variations in the individual station teleseismic P-wave  $m_b$  magnitude of up to 0.3 magnitude units. However these magnitude variations should be substantially reduced by averaging over stations at multiple azimuths.

The reverberant coda appears to arise from scattered modal waves that are initially excited in the low velocity near-surface structures of the Yucca Flats deposits of alluvium and tuff. Scattering of the waves occurs at offsets in the basement structure and the at the sides of the valley.

The combined effects of scattering, source function, intrinsic attenuation, and instrument response serve to obscure the P+pP spectral scalloping that is expected from a linear model. This loss of spectral resolution is the product of P coda filling in the P+pP interference notches and the lengthening of the initial P wave source time function by the convolution of the source time function, intrinsic attenuation operator and instrument response. Therefore, short time windows that do not include P coda energy do not have sufficient resolution to reliably detect the P+pP interference notches.

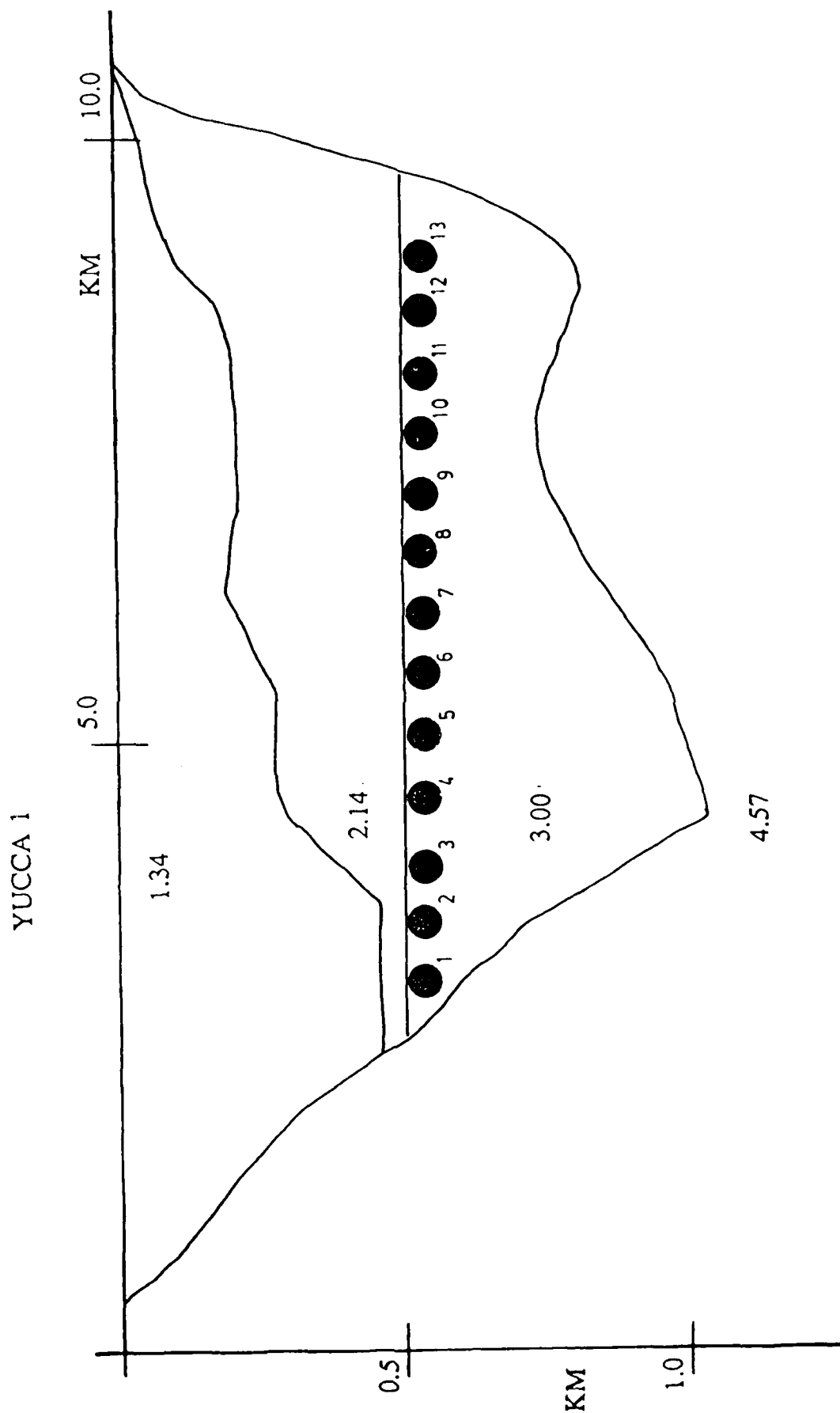


Figure 4.1 West-to-East model for geologic structure across Yucca Flats from Ferguson (1983). Model shown with 5-to-1 vertical exaggeration. Numbered source locations referred to in the text are indicated by solid dots at a depth of 550 meters below the surface. P-wave velocities of 1.34, 2.14, 3.00, and 4.57 km/sec are indicated for the geologic units of alluvium, unsaturated tuff, saturated tuff, and Paleozoic carbonates respectively.

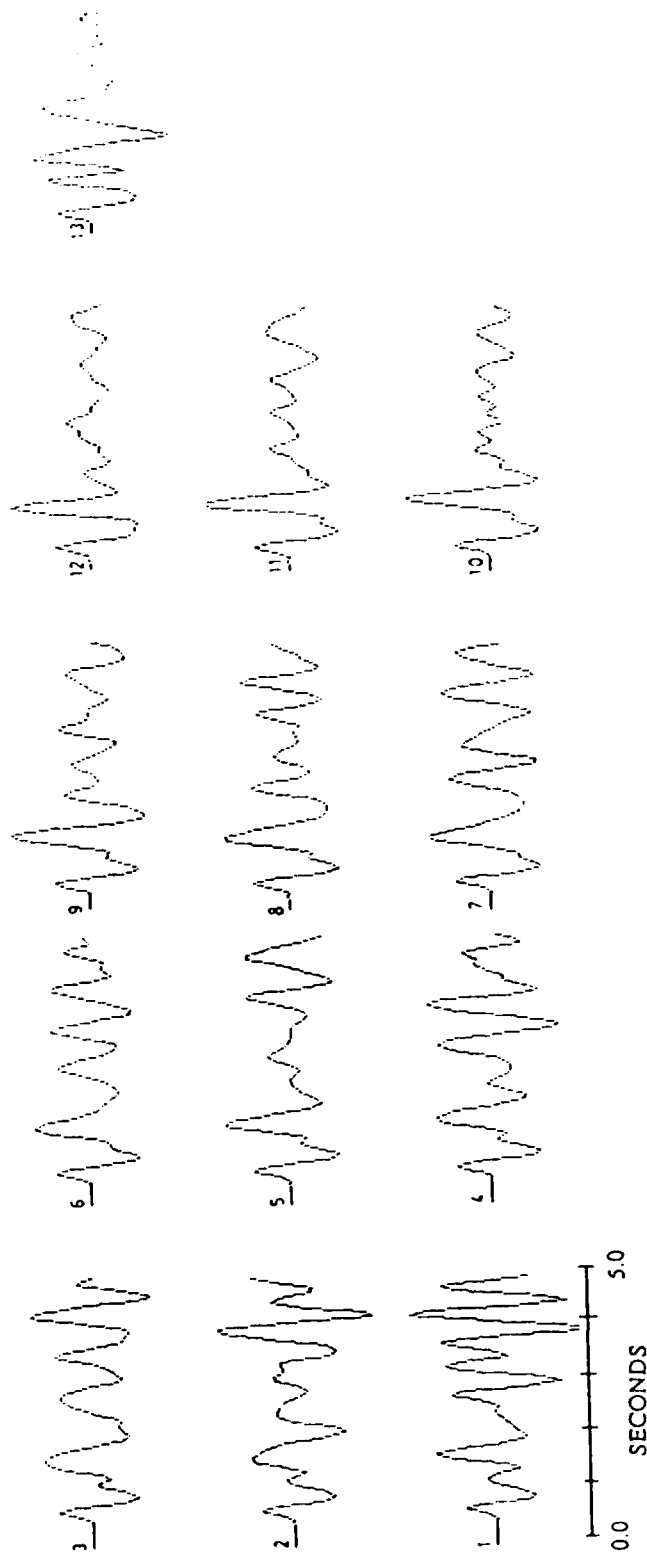


Figure 4.2 Teleseismic P-wave synthetics appropriate for a takeoff angle of 15 degrees for model in Figure 1. Numbers correspond to numbered source locations in Figure 1. 5 seconds of record are shown in each case. All synthetics are plotted at the same scale. Synthetics are calculated for a von Seggern Blandford (1972) hard rock 100 Kt RDP convolved with an instrument response and an attenuation operator as in FIGURE 2.

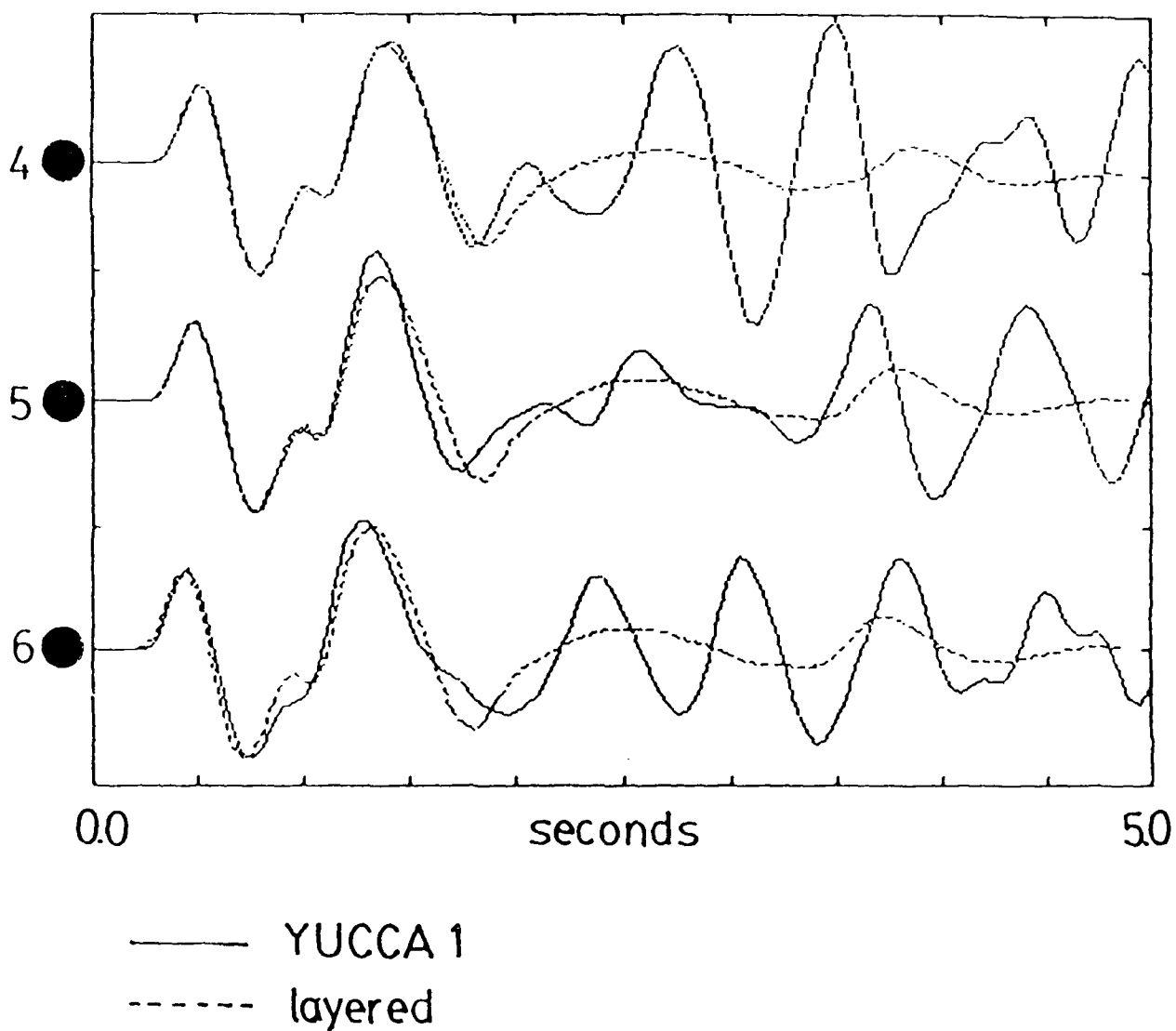


Figure 4.3 Synthetics for source locations 4, 5, and 6 at takeoff angle of 15 degrees compared to the layered model.

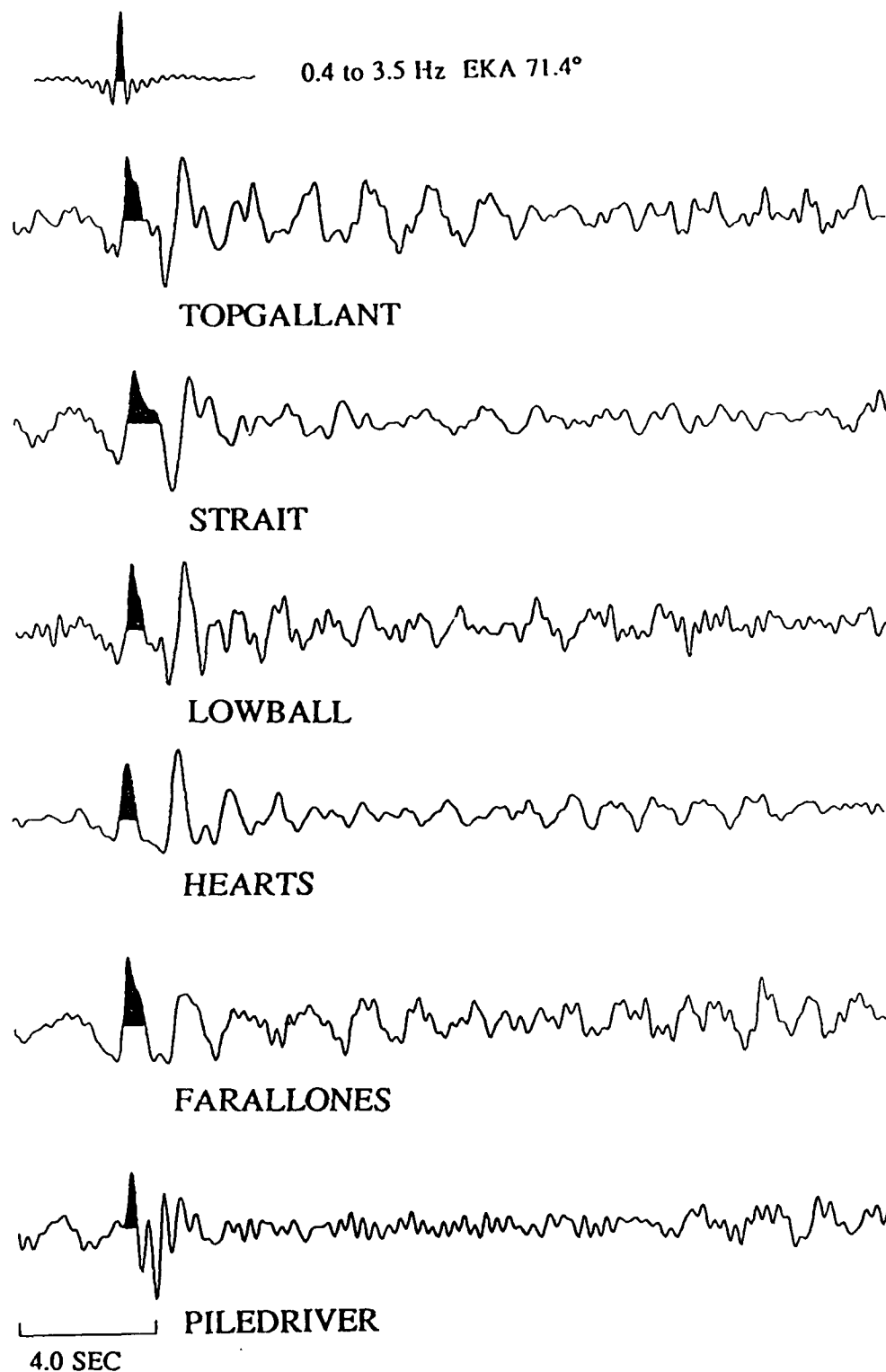


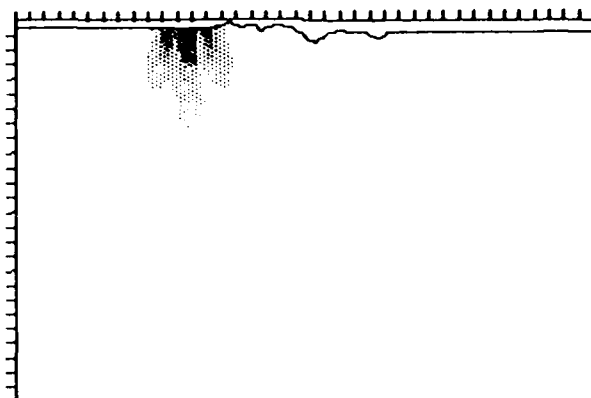
Figure 4.4 Deconvolved source time functions (far-field displacement) of Yucca Flats events and Piledriver at EKA array ( $\Delta=71.4^\circ$ ). The effects of a constant  $t^*=0.45$  sec attenuation operator have been removed. A resolution kernel is shown at the top representing the limited bandwidth of the deconvolutions, 0.4 to 3.5 Hz. The initial causal P wave has been shaded for clarity. Note the higher frequency and shorter duration source time function of Piledriver with respect to the Yucca Flats events. Topgallant, Lowball, and Farallones have considerable reverberation in the first 5 seconds of record. The Yucca Flats events do not show a clear pP within 1 second of the initial P wave, although several events do show a negative phase about 1 second following the P wave and a positive pulse about 1.5 seconds following the P wave. Piledriver shows a negative pulse about 0.25 seconds following the P wave (pP?) and another negative polarity pulse about 0.8 seconds following the P wave.

## FINITE-DIFFERENCE SIMULATIONS OF RAYLEIGH WAVE SCATTERING BY 2-D ROUGH TOPOGRAPHY

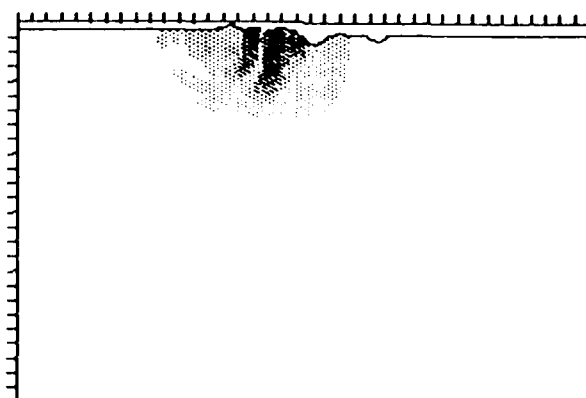
Keith Lynn McLaughlin and Rong-Song Jih  
Teledyne Geotech Alexandria Labs  
314 Montgomery Street  
Alexandria, Virginia 22314-1581

### ABSTRACT

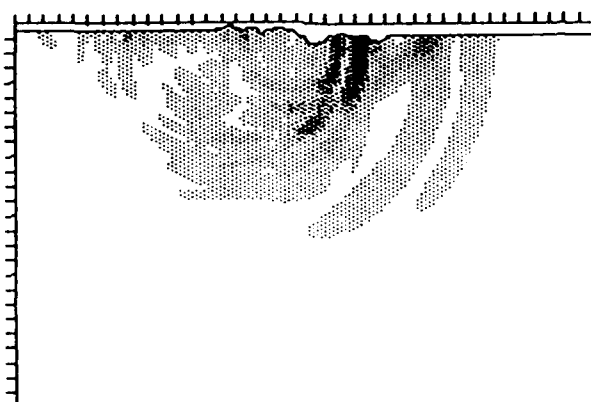
Rayleigh waves normally incident upon 2-D simple or rough topographic structures are simulated by the linear finite-difference method to study the attenuation, transmission, and reflection of Rayleigh waves and to measure the Rayleigh-to-P and -SV bodywave conversion. For simple ramp structures, transmission, reflection, and scattering depend on the sign of change of slope of the topographic feature, as well as the ratio of the ramp height to the wavelength,  $h/\lambda$ . Simple ramp structures produce back-scattered bodywaves for  $h > \lambda$ , and forward-scattered bodywaves for  $h < \lambda$ . The radiation patterns of P and S bodywaves are roughly consistent with the model of equivalent point forces along the free surface. More complicated topographic features generated by random Markov sequences have been characterized by the Rayleigh-wave spatial  $Q(f)$ . As expected, rougher topography attenuates Rayleigh waves more than smooth topography. P and S amplitudes ratios are consistent with radiation from equivalent point forces near the surface, but the distribution of slownesses generated is greater than from the simple ramp structures. Reflection of Rayleigh waves by topographic slopes and by random topography is an inefficient process and the bulk of the energy that is not transmitted as Rayleigh waves is converted to bodywaves. Fundamental Rayleigh-to-Lg scattering and generation of teleseismic P coda by short period Rayleigh should be observable.



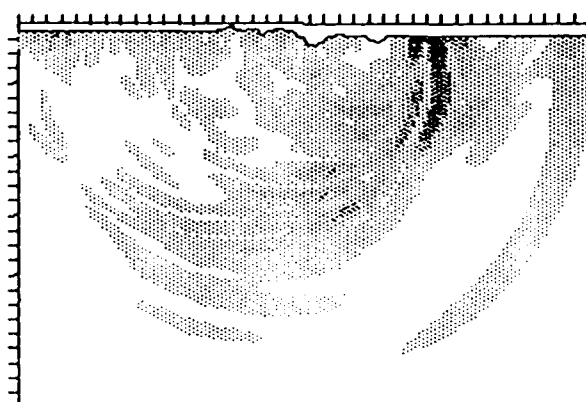
(A)



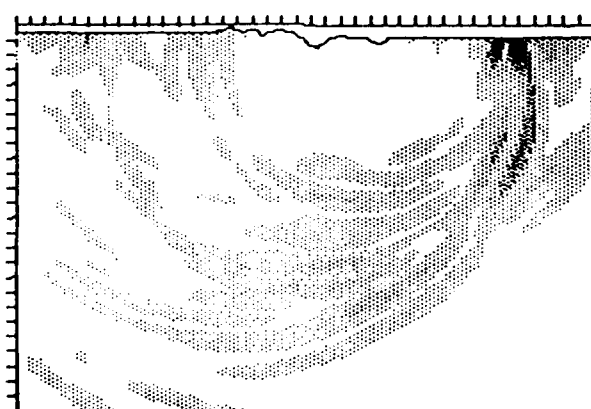
(B)



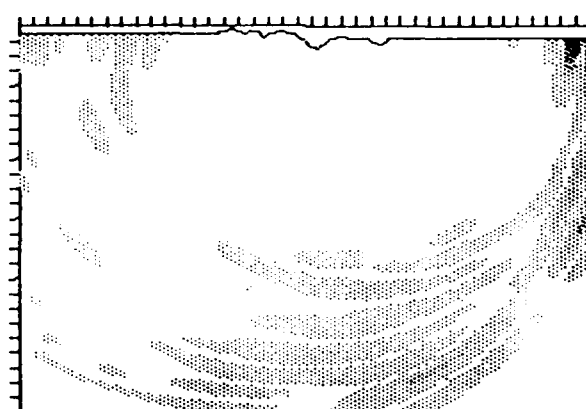
(C)



(D)

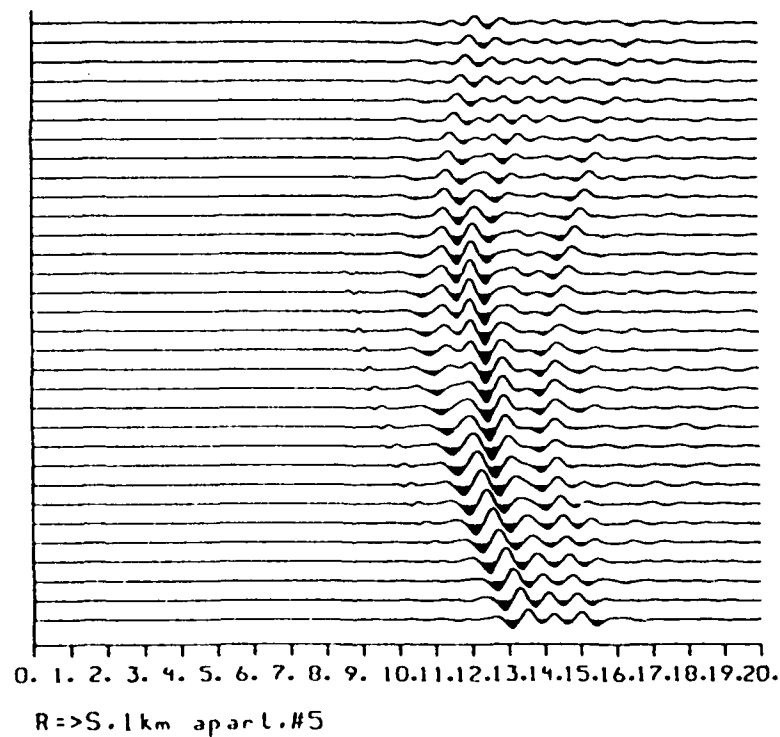
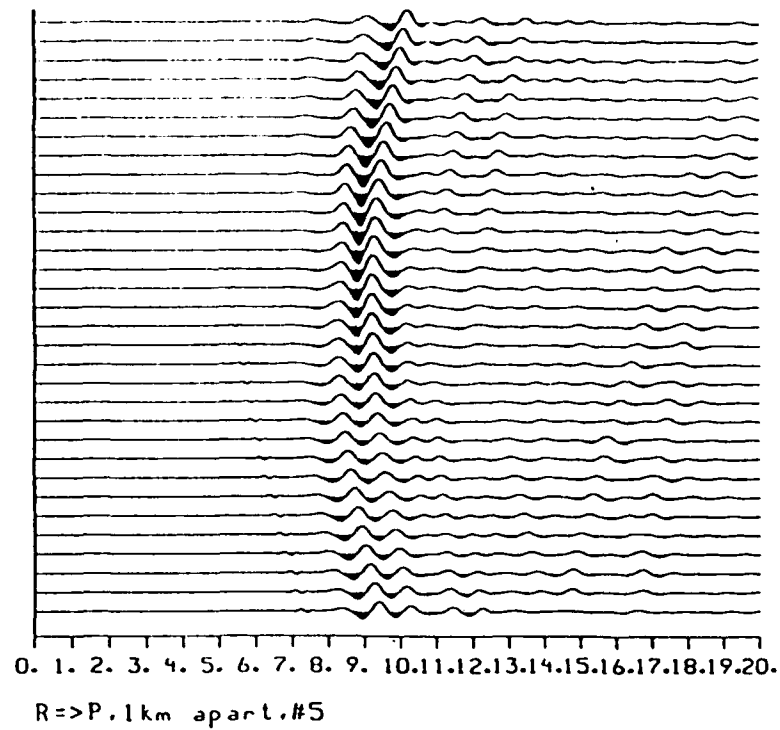


(E)



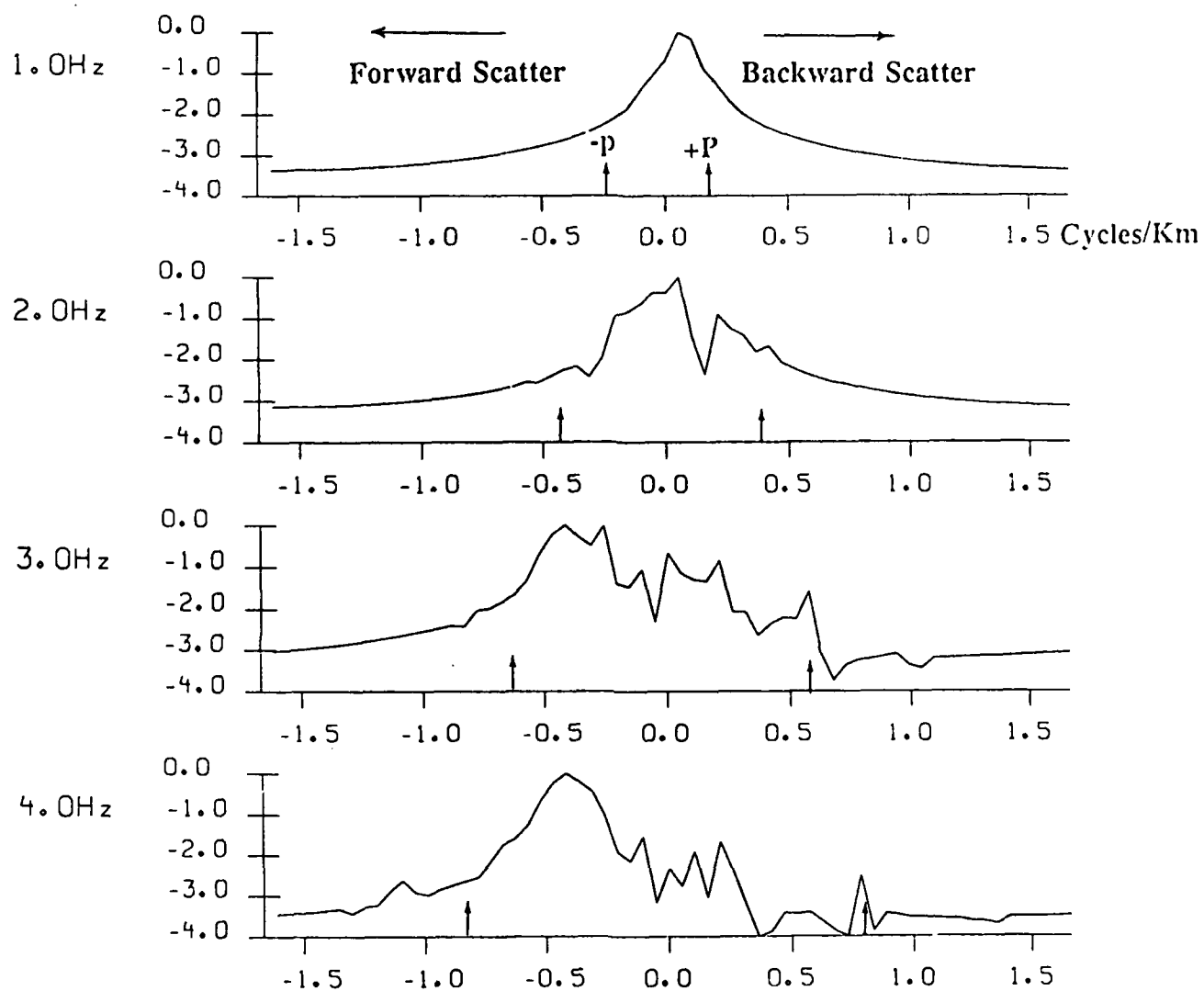
(F)

Figure 5.1 Rayleigh wave incident on a rough topographic profile superimposed on a grid with absorbing boundary conditions for the sides and the bottom. Figures (A) through (F) correspond to displacement wavefields at distinct times with a temporal spacing of 2 sec. Note that the high frequency scattering of Rayleigh wave is *forward*.



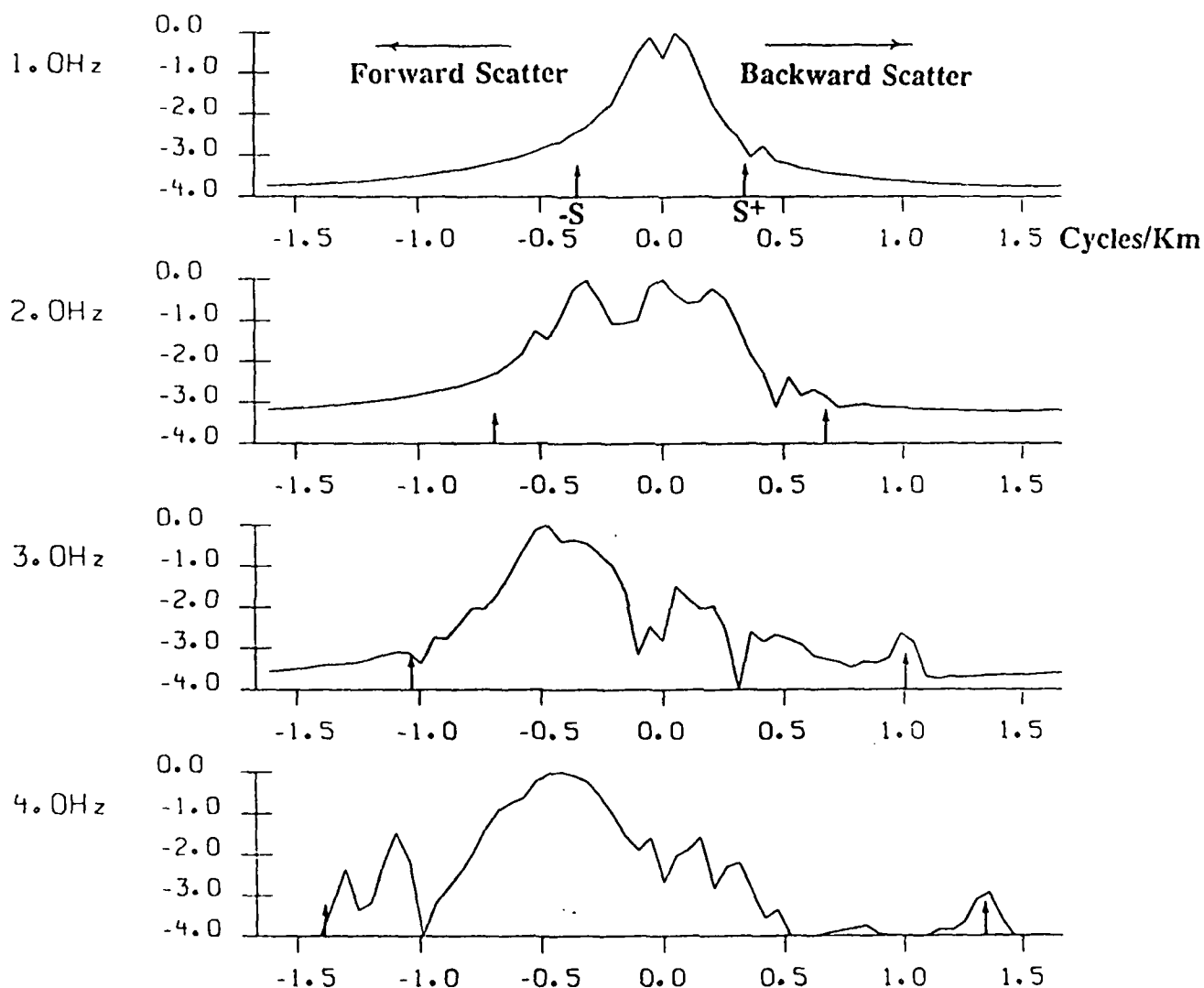
**Figure 5.2** Seismic sections recording the converted P wave (dilatational strain, upper) and S wave (rotational strain, below) at a line of 32 sensors located near the bottom of the grid spaced 1 km apart for the same rough topography (#5) as in previous figure. Complicated interference patterns are evident for both P and S wavefields.





### NORMALIZED $\text{Log}(\text{POWER})$ WAVENUMBER SPECTRA

Figure 5.3 Frequency wavenumber spectra for the dilatational strain field (P-wave) recorded near the bottom of the grid with topography #5 on the top of the grid. The dilatational strain energy is largely confined to P wave slowness across the array. P wave energy shifts from back-scattered to forward-scattered from 1 to 4 Hz.



### NORMALIZED $\text{Log}(\text{POWER})$ WAVENUMBER SPECTRA

Figure 5.4 Frequency wavenumber spectra for the rotational strain field (S-wave) recorded near the bottom of the grid with topography #5 on the top. The rotational strain energy is largely confined to S wave slowness across the array. S wave energy shifts from back-scattered to forward-scattered from 1 to 4 Hz.

DISTRIBUTION LIST

Dr. Monem Abdel-Gawad  
Rockwell International Science Center  
1049 Camino Dos Rios  
Thousand Oaks, CA 91360

Professor Keiiti Aki  
Center for Earth Sciences  
University of Southern California  
University Park  
Los Angeles, CA 90089-0741

Professor Shelton S. Alexander  
Geosciences Department  
403 Deike Building  
The Pennsylvania State University  
University Park, PA 16802

Professor Charles B. Archambeau  
Cooperative Institute for Research in  
Environmental Sciences  
University of Colorado  
Boulder, CO 80309

Dr. Thomas C. Bache Jr.  
Science Applications Int'l Corp.  
10210 Campus Point Drive  
San Diego, CA 92121

Dr. James Bulau  
Rockwell International Science Center  
1049 Camino Dos Rios  
P.O. Box 1085  
Thousand Oaks, CA 91360

Dr. Douglas R. Baumgardt  
Signal Analysis and Systems Division  
ENSCO, Inc.  
5400 Port Royal Road  
Springfield, VA 22151-2388

Dr. S. Bratt  
Science Applications Int'l Corp.  
10210 Campus Point Drive  
San Diego, CA 92121

Professor John Ebel  
Department of Geology & Geophysics  
Boston College  
Chestnut Hill, MA 02167

Woodward-Clyde Consultants  
Attn: Dr. Lawrence J. Burdick  
Dr. Jeff Barker  
P.O. Box 93245  
Pasadena, CA 91109-3245 (2 copies)

Dr. Roy Burger  
1221 Serry Rd.  
Schenectady, NY 12309

Professor Robert W. Clayton  
Seismological Laboratory  
Division of Geological and Planetary  
Sciences  
California Institute of Technology  
Pasadena, CA 91125

Dr. Vernon F. Cormier  
Earth Resources Laboratory  
Department of Earth, Atmospheric and  
Planetary Sciences  
Massachusetts Institute of Technology  
42 Carleton Street  
Cambridge, MA 02142

Professor Anton M. Dainty  
Earth Resources Laboratory  
Department of Earth, Atmospheric and  
Planetary Sciences  
Massachusetts Institute of Technology  
42 Carleton Street  
Cambridge, MA 02142

Dr. Zoltan A. Der  
Teledyne Geotech  
314 Montgomery Street  
Alexandria, VA 22314

Prof. Adam Dziewonski  
Hoffman Laboratory  
Harvard University  
20 Oxford St.  
Cambridge, MA 02138

Professor John Ferguson  
Center for Lithospheric Studies  
The University of Texas at Dallas  
P.O. Box 830688  
Richardson, TX 75083-0688

Dr. Jeffrey W. Given  
Sierra Geophysics  
11255 Kirkland Way  
Kirkland, WA 98033

Prof. Roy Greenfield  
Geosciences Department  
403 Deike Building  
The Pennsylvania State University  
University Park, PA 16802

Professor David G. Harkrider  
Seismological Laboratory  
Division of Geological and Planetary  
Sciences  
California Institute of Technology  
Pasadena, CA 91125

Professor Donald V. Helmberger  
Seismological Laboratory  
Division of Geological and Planetary  
Sciences  
California Institute of Technology  
Pasadena, CA 91125

Professor Eugene Herrin  
Institute for the Study of Earth & Man  
Geophysical Laboratory  
Southern Methodist University  
Dallas, TX 75275

Professor Robert B. Herrmann  
Department of Earth and Atmospheric  
Sciences  
Saint Louis University  
Saint Louis, MO 63156

Professor Lane R. Johnson  
Seismographic Station  
University of California  
Berkeley, CA 94720

Professor Thomas H. Jordan  
Department of Earth, Atmospheric and  
Planetary Sciences  
Massachusetts Institute of Technology  
Cambridge, MA 02139

Dr. Alan Kafka  
Department of Geology & Geophysics  
Boston College  
Chestnut Hill, MA 02167

Professor Charles A. Langston  
Geosciences Department  
403 Deike Building  
The Pennsylvania State University  
University Park, PA 16802

Professor Thorne Lay  
Department of Geological Sciences  
1006 C.C. Little Building  
University of Michigan  
Ann Arbor, MI 48109-1063

Dr. George R. Mellman  
Sierra Geophysics  
11255 Kirkland Way  
Kirkland, WA 98033

Professor Brian J. Mitchell  
Department of Earth and Atmospheric  
Sciences  
Saint Louis University  
Saint Louis, MO 63156

Professor Thomas V. McEvilly  
Seismographic Station  
University of California  
Berkeley, CA 94720

Dr. Keith L. McLaughlin  
Teledyne Geotech  
314 Montgomery Street  
Alexandria, VA 22314

Professor Otto W. Nuttli  
Department of Earth and Atmospheric  
Sciences  
Saint Louis University  
Saint Louis, MO 63156

Professor Paul G. Richards  
Lamont-Doherty Geological Observatory  
of Columbia University  
Palisades, NY 10964

Dr. Norton Rimer  
S-Cubed  
A Division of Maxwell Laboratory  
P.O. 1620  
La Jolla, CA 92038-1620

Professor Larry J. Ruff  
Department of Geological Sciences  
1006 C.C. Little Building  
University of Michigan  
Ann Arbor, MI 48109-1063

Professor Charles G. Sammis  
Center for Earth Sciences  
University of Southern California  
University Park  
Los Angeles, CA 90089-0741

Dr. David G. Simpson  
Lamont-Doherty Geological Observatory  
of Columbia University  
Palisades, NY 10964

Dr. Jeffrey L. Stevens  
S-CUBED,  
A Division of Maxwell Laboratory  
P.O. Box 1620  
La Jolla, CA 92038-1620

Professor Brian Stump  
Institute for the Study of Earth  
and Man  
Geophysical Laboratory  
Southern Methodist University  
Dallas, TX 75275

Professor Ta-liang Teng  
Center for Earth Sciences  
University of Southern California  
University Park  
Los Angeles, CA 90089-0741

Dr. R. B. Tittmann  
Rockwell International Science Center  
1049 Camino Dos Rios  
P.O. Box 1085  
Thousand Oaks, CA 91360

Professor M. Nafi Toksoz  
Earth Resources Laboratory  
Department of Earth, Atmospheric and  
Planetary Sciences  
Massachusetts Institute of Technology  
42 Carleton Street  
Cambridge, MA 02142

Professor Terry C. Wallace  
Department of Geosciences  
Building #11  
University of Arizona  
Tucson, AZ 85721

Prof. John H. Woodhouse  
Hoffman Laboratory  
Harvard University  
20 Oxford St.  
Cambridge, MA 02138

Dr. G. Blake  
US Dept of Energy/DP 331  
Forrestal Building  
1000 Independence Ave.  
Washington, D.C. 20585

Dr. Michel Bouchon  
Universite Scientifique et  
Medicale de Grenoble  
Laboratoire de Geophysique  
Interne et Tectonophysique  
I.R.I.G.M.-B.P. 68  
38402 St. Martin D'Herès  
Cedex FRANCE

Dr. Hilmar Bungum  
NTNF/NORSAR  
P.O. Box 51  
Norwegian Council of Science,  
Industry and Research, NORSAR  
N-2007 Kjeller, NORWAY

Dr. Alan Douglas  
Ministry of Defense  
Blacknest, Brimpton, Reading RG7-4RS  
UNITED KINGDOM

Professor Peter Harjes  
Institute for Geophysik  
Rhur University  
Bochum  
P.O. Box 102148  
4630 Bochum 1  
FEDERAL REPUBLIC OF GERMANY

Dr. James Hannon  
Lawrence Livermore National Laboratory  
P.O. Box 808  
Livermore, CA 94550

Dr. E. Husebye  
NTNF/NORSAR  
P.O. Box 51  
N-2007 Kjeller, NORWAY

Dr. Arthur Lerner-Lam  
Lamont-Doherty Geological Observatory  
of Columbia University  
Palisades, NY 10964

Mr. Peter Marshall  
Procurement Executive  
Ministry of Defense  
Blacknest, Brimpton, Reading RG7-4RS  
UNITED KINGDOM

Dr. B. Massinon  
Societe Radiomana  
27, Rue Claude Bernard  
75005, Paris, FRANCE

Dr. Pierre Mechler  
Societe Radiomana  
27, Rue Claude Bernard  
75005, Paris, FRANCE

Mr. Jack Murphy  
S-CUBED  
Reston Geophysics Office  
11800 Sunrise Valley Drive  
Suite 1212  
Reston, VA 22091

Dr. Svein Mykkeltveit  
NTNF/NORSAR  
P.O. Box 51  
N-2007 Kjeller, NORWAY

Dr. Carl Newton  
Los Alamos National Laboratory  
P.O. Box 1663  
Mail Stop C 335, Group ESS3  
Los Alamos, NM 87545

Dr. Peter Basham  
Earth Physics Branch  
Department of Energy and Mines  
1 Observatory Crescent  
Ottawa, Ontario  
CANADA K1A 0Y3

Professor J. A. Orcutt  
Geological Sciences Division  
Univ. of California at San Diego  
La Jolla, CA 92093

Dr. Frank F. Pilotte  
Director of Geophysics  
Headquarters Air Force Technical  
Applications Center  
Patrick AFB, Florida 32925-6001

Professor Keith Priestley  
University of Nevada  
Mackay School of Mines  
Reno, Nevada 89557

Mr. Jack Raclin  
USGS - Geology, Rm 3C136  
Mail Stop 928 National Center  
Reston, VA 22092

Dr. Frode Ringdal  
NTNF/NORSAR  
P.O. Box 51  
N-2007 Kjeller, NORWAY

Dr. George H. Rothe  
Chief, Research Division  
Geophysics Directorate  
Headquarters Air Force Technical  
Applications Center  
Patrick AFB, Florida 32925-6001

Dr. Alan S. Ryall, Jr.  
Center for Seismic Studies  
1300 North 17th Street  
Suite 1450  
Arlington, VA 22209-2308

Dr. Lawrence Turnbull  
OSWR/NED  
Central Intelligence Agency  
CIA, Room 5G48  
Washington, DC 20505

Professor Steven Grand  
Department of Geology  
245 Natural History Bldg  
1301 West Green Street  
Urbana, IL 61801

DARPA/PM  
1400 Wilson Boulevard  
Arlington, VA 22209

U.S. Geological Survey  
ATTN: Dr. T. Hanks  
National Earthquake Research Center  
345 Middlefield Road  
Menlo Park, CA 94025

Defense Technical Information Center  
Cameron Station  
Alexandria, VA 22314 (12 copies)

SRI International  
333 Ravensworth Avenue  
Menlo Park, CA 94025

Defense Intelligence Agency  
Directorate for Scientific and  
Technical Intelligence  
Washington, D.C. 20301

Center for Seismic Studies  
ATTN: Dr. C. Romney  
1300 North 17th Street  
Suite 1450  
Arlington, VA 22209 (3 copies)

Defense Nuclear Agency  
Shock Physics Directorate/SS  
Washington, D.C. 20305

Dr. Robert Blandford  
DARPA/GSD  
1400 Wilson Boulevard  
Arlington, VA 22209-2308

Defense Nuclear Agency/SPSS  
ATTN: Dr. Michael Shore  
6801 Telegraph Road  
Alexandria, VA 22310

Ms. Ann Kerr  
DARPA/GSD  
1400 Wilson Boulevard  
Arlington, VA 22209-2308

AFOSR/NPG  
ATTN: Director  
Bldg 410, Room C222  
Bolling AFB, Washington, D.C. 20332

Dr. Ralph Alewine III  
DARPA/GSD  
1400 Wilson Boulevard  
Arlington, VA 22209-2308

AFTAC/CA (STINFO)  
Patrick AFB, FL 32925-6001

Mr. Edward Giller  
Pacific Sierra Research Corp.  
1401 Wilson Boulevard  
Arlington, VA 22209

AFWL/NTESC  
Kirtland AFB, NM 87171

Science Horizons, Inc.  
Attn: Dr. Bernard Minster  
Dr. Theodore Cherry  
710 Encinitas Blvd., Suite 101  
Encinitas, CA 92024 (2 copies)

U.S. Arms Control & Disarmament Agency  
ATTN: Mrs. M. Hoinkes  
Div. of Multilateral Affairs, Rm 5499  
Washington, D.C. 20451

Dr. Jack Evernden  
USGS - Earthquake Studies  
345 Middlefield Road  
Menlo Park, CA 94025

Dr. Lawrence Braile  
Department of Geosciences  
Purdue University  
West Lafayette, IN 47907

Dr. G.A. Bollinger  
Department of Geological Sciences  
Virginia Polytechnical Institute  
21044 Derring Hall  
Blacksburg, VA 24061

Dr. L. Sykes  
Lamont Doherty Geological Observatory  
Columbia University  
Palisades, NY 10964

Dr. S.W. Smith  
Geophysics Program  
University of Washington  
Seattle, WA 98195

Dr. L. Timothy Long  
School of Geophysical Sciences  
Georgia Institute of Technology  
Atlanta, GA 30332

Dr. N. Biswas  
Geophysical Institute  
University of Alaska  
Fairbanks, AK 99701

Dr. Freeman Gilbert  
Institute of Geophysics &  
Planetary Physics  
Univ. of California at San Diego  
P.O. Box 109  
La Jolla, CA 92037

Dr. Pradeep Talwani  
Department of Geological Sciences  
University of South Carolina  
Columbia, SC 29208

University of Hawaii  
Institute of Geophysics  
Attn: Dr. Daniel Walker  
Honolulu, HI 96822

Dr. Donald Forsyth  
Department of Geological Sciences  
Brown University  
Providence, RI 02912

Dr. Jack Oliver  
Department of Geology  
Cornell University  
Ithaca, NY 14850

Dr. Muawia Barazangi  
Geological Sciences  
Cornell University  
Ithaca, NY 14853

Rondout Associates  
Attn: Dr. George Sutton  
Dr. Jerry Carter  
Dr. Paul Pomeroy  
P.O. Box 224  
Stone Ridge, NY 12484 (3 copies)

Dr. M. Sorrells  
Geotech/Teledyne  
P.O. Box 28277  
Dallas, TX 75228

Dr. Bob Smith  
Department of Geophysics  
University of Utah  
1400 East 2nd South  
Salt Lake City, UT 84112

Dr. Anthony Gangi  
Texas A&M University  
Department of Geophysics  
College Station, TX 77843

Dr. Gregory B. Young  
ENSCO, Inc.  
5400 Port Royal Road  
Springfield, CA 22151

Dr. Ben Menaheim  
Weizman Institute of Science  
Rehovot, ISRAEL 951729

Weidlinger Associates  
Attn: Dr. Gregory Wojcik  
620 Hansen Way, Suite 100  
Palo Alto, CA 94304

Dr. Leon Knopoff  
University of California  
Institute of Geophysics & Planetary  
Physics  
Los Angeles, CA 90024

Dr. Kenneth H. Olsen  
Los Alamos Scientific Laboratory  
Post Office Box 1663  
Los Alamos, NM 87545



Prof. Jon F. Claerbout  
Prof. Amos Nur  
Dept. of Geophysics  
Stanford University  
Stanford, CA 94305 (2 copies)

Dr. Robert Burridge  
Schlumberger-Doll Research Ctr.  
Old Quarry Road  
Ridgefield, CT 06877

Dr. Eduard Berg  
Institute of Geophysics  
University of Hawaii  
Honolulu, HI 96822

Dr. Robert Phinney  
Dr. F.A. Dahlen  
Dept. of Geological & Geophysical Sci.  
Princeton University  
Princeton, NJ 08540 (2 copies)

Dr. Kin-Yip Chun  
Geophysics Division  
Physics Department  
University of Toronto  
Ontario, CANADA M5S 1A7

New England Research, Inc.  
Attn: Dr. Randolph Martin III  
P.O. Box 857  
Norwich, VT 05055

Sandia National Laboratory  
Attn: Dr. H.B. Durham  
Albuquerque, NM 87185

Dr. Gary McCartor  
Mission Research Corp.  
735 State Street  
P. O. Drawer 719  
Santa Barbara, CA 93102

Dr. W. H. K. Lee  
USGS  
Office of Earthquakes, Volcanoes,  
& Engineering  
Branch of Seismology  
345 Middlefield Rd  
Menlo Park, CA 94025

AFGL/XO  
Hanscom AFB, MA 01731-5000

AFGL/LW  
Hanscom AFB, MA 01731-5000

AFGL/SULL  
Research Library  
Hanscom AFB, MA 01731-5000 (2 copies)

Secretary of the Air Force (SAFRD)  
Washington, DC 20330

Office of the Secretary Defense  
DDR & E  
Washington, DC 20330

HQ DNA  
Attn: Technical Library  
Washington, DC 20305

Director, Technical Information  
DARPA  
1400 Wilson Blvd.  
Arlington, VA 22209

Los Alamos Scientific Laboratory  
Attn: Report Library  
Post Office Box 1663  
Los Alamos, NM 87544

Dr. Thomas Weaver  
Los Alamos Scientific Laboratory  
Los Alamos, NM 87544

Dr. Al Florence  
SRI International  
333 Ravenswood Avenue  
Menlo Park, CA 94025-3493

END

7-87

DTIC